

Responses to Reviewer #1

First of all, we would like to thank the reviewer for this positive assessment of our manuscript, the constructive and helpful suggestions. Point-to-point responses are given below. The original comments are black in color, while our responses are in blue. All the mentioned line number are referred to the revised manuscript.

Major comments

The new method is based on the aerosol optical properties, which is summarized from the measurements. So I suggested the authors can present some evidences of theoretical estimation with the forward RTM to enhanced the principle basis of the method somewhere, even in the supplementary materials.

R: Thanks for your great suggestion. In order to enhance the principle basis of this method described in the manuscript, we used radiative transfer model of SCIATRAN to simulate O₄ DSCDs in UV and Visible bands under conditions with different aerosol optical properties. As listed in Table R1, 11 different aerosol scenarios were simulated in total, in which case 1 is the default case to represent haze condition. Case 1 to 7 describe the aerosol scenarios of gradually increase of scattering properties with a fixed σ_{abs} of 0.050 km⁻¹, which cause the growths in both extinction and SSA. Case 8 to 11 present another process of the gradually increase of haze with more absorbing aerosols under the condition that σ_{sca} are fixed on 0.250 km⁻¹, which consequently result in an increase extinction but decrease of SSA.

Table 1. Simulation-based correlation information between O₄ DSCDs at 360.8 and 477.1 nm under conditions with different aerosol optical properties.

Aerosol information					Slope	R ²	Intercept
No.	σ_{abs}	σ_{sca}	σ_{ext}	SSA			
1	0.050	0.075	0.125	0.6000	0.9560	0.9968	0.5516
2	0.050	0.125	0.175	0.7143	0.9117	0.9859	0.3178
3	0.050	0.250	0.300	0.8333	0.8089	0.9087	0.1438
4	0.050	0.350	0.400	0.8750	0.5672	0.8842	0.3861
5	0.050	0.500	0.550	0.9091	0.5649	0.9800	0.2305
6	0.050	0.700	0.750	0.9333	0.4519	0.9447	0.2603
7	0.050	1.000	1.050	0.9524	0.4875	0.9979	0.1654
8	0.010	0.250	0.260	0.9615	0.6754	0.7963	0.3948
9	0.025	0.250	0.275	0.9091	0.7682	0.9138	0.2353
10	0.075	0.250	0.325	0.7692	0.8051	0.9007	0.1407
11	0.100	0.250	0.350	0.7143	0.8446	0.9063	0.1011

Then, we did the linear-regression analysis for the simulated UV and Visible O₄ DSCDs under different aerosol conditions. As shown in Figure R1, the slope and R² between UV and Visible O₄ DSCDs illustrate that:

- (1) Case 1-7 show an exponential trend in Figure R1. The fitting slope decrease accompanied with the increase of extinction coefficients and SSA if the condition of absorption coefficients are determined.
- (2) Case 8-11 show a linear trend in Figure R1. The fitting slope will decrease

together with the decrease of extinction coefficients and the increase of SSA when the condition of absorption coefficients are determined.

- (3) The correlation coefficients are high (R^2 are mainly greater than 0.90) for all the simulation results. As shown in case 8-11, R^2 decrease accompanied with the decrease of the correlation slopes. This conclusion need to be further supported by more detailed simulations.

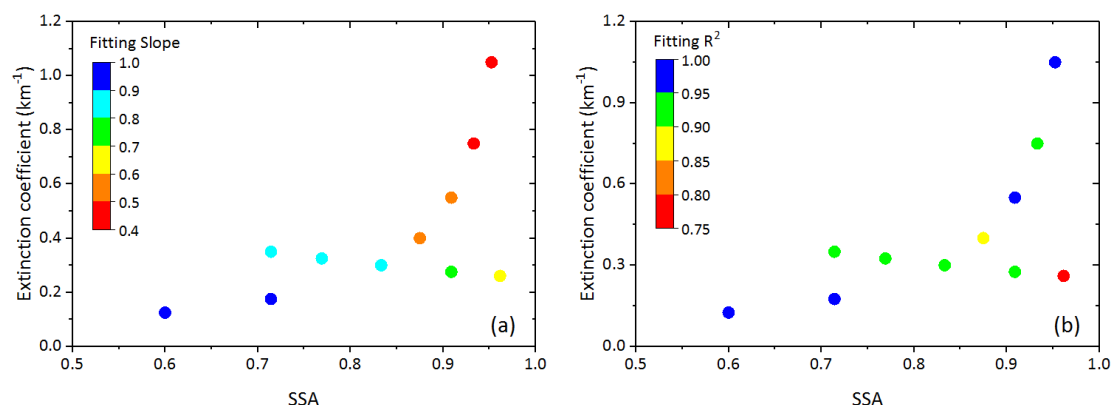


Figure R1. Correlation information (fitting slope and R^2) of the linear regression analysis between the simulated O₄ DCSDs at 360.8 and 477.1 nm under conditions of different aerosol optical properties in the simulation sensitivity studies.

The forward RTM simulation results could demonstrate that the O₄ absorptions (the value of UV and Visible O₄ DSCDs, the corresponding linear-regression slope and R^2 between them) could greatly reflect the variation of aerosol optical properties, which present the theoretical evidences to some extent and enhance the principle basis of the proposed method. Moreover, the simulation results are consistent with the conclusions in the manuscript. The more detailed simulations in the future could provide the better quantitative relationship to the aerosol properties even more.

In addition, we have added this section to Discussion and the Supplement. Please refer to 333-339 in the manuscript.

Minor comments

(1) P4, Sect. 2.2 & P5, Fig. 1 => Please provide the basic information of the measured spectrum in the fitting example, which can be help to evaluate the performance of spectral analysis better.

R: The Fig. 1 in manuscript presents the typical spectral fitting of O₄ DSCDs in UV and Visible bands, and the corresponding measured spectrum were collected at 09:57:29 (SZA (Solar Zenith Angle) = 66.67°, SAA (Solar Azimuth Angle) = 48.40°, ELE (Elevation Angle) = 10°) and 09:42:29 (SZA = 68.27°, SAA = 49.29° and ELE = 5°) on 22 November 2016, respectively. We have supplemented the measured spectra information in the Fig. 1.

Besides, the completed spectral fitting were shown in Fig. R2 here.

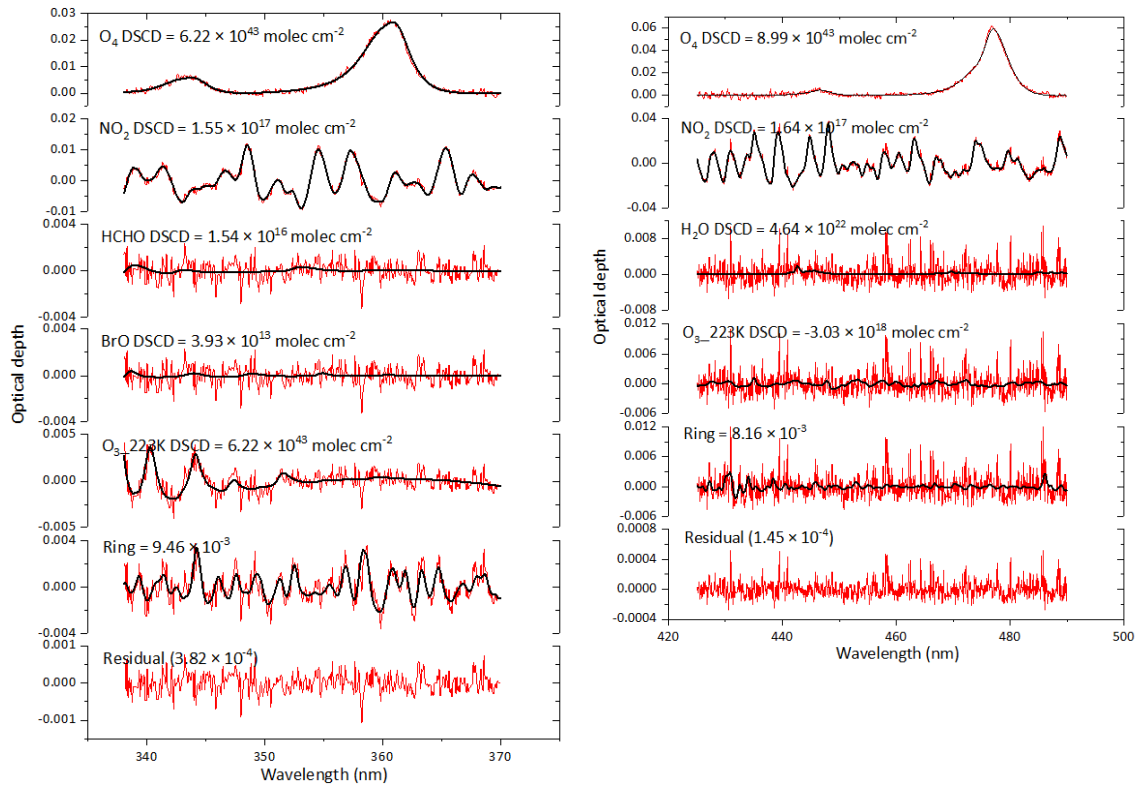


Figure R2. Example of DOAS spectral fitting of O_4 DSCDs in UV (left) and Vis (right) band. Black lines represent the absorption signal and red lines represent the sum of the absorption signal and the fit residual. The example spectrum used to retrieve UV and Visible O_4 DSCDs were obtained at 09:57:29 and 09:42:29 on 22 November 2016, respectively.

(2) P8, L161-165 => Any special consideration for using different RH for clear days, non-haze days ($RH < 80\%$) with haze days ($RH \leq 80\%$)?

R: We apologized for this mistake of typing. In fact, we use $RH < 80\%$ to determine haze and heavy-haze days. In other words, RH all should be $< 80\%$ for clear, non-haze, haze and heavy-haze days. We have corrected this in the revised manuscript.

(3) P10, Fig.3 => Besides the discussion about the correlation coefficient, could the authors give some explanations of the changes in slopes among different weather types? Obviously, the slope in clear and non-haze days are much larger than those in haze and heavy-haze days. Why?

R: The oxygen collision complexes O_4 vertical profiles is well known and nearly constant in the atmosphere, the observed O_4 absorption can serve as an indicator for the atmospheric distribution of photon paths (Wagner et al., 2004; Frieß et al., 2006). The O_4 differential slant column densities (DSCDs) measured by MAX-DOAS are mainly attributed to the photon paths. Since the existence of aerosol can change the light path a lot, the variation of aerosol vertical profiles will be the main factor influencing the photon paths in a cloud-free sunny day, which will be further reflected in the observed O_4 DSCDs.

The path lengths from the effective scattering event to the telescope are dependent on

wavelengths. The path length in visible ranges is obviously longer than that in ultraviolet ranges. In clear and non-haze days, the path length is slightly affected by aerosols. However, the significant increasing of aerosol extinction coefficients in haze and heavy-haze days will have a large effect on the reduction in light path lengths. The reduced light path lengths are thought to result in small O_4 DSCDs. If these light path lengths are sufficiently shortened to penetrate hazy atmosphere, the measured O_4 DSCDs have large uncertainties and may lose sensitivity to vertical distributions of aerosol load (Lee et al., 2011). That could be the reason for the correlation slope in clear and non-haze days are much larger than those in haze and heavy-haze days. Moreover, as shown in Figure R3, the simulation results could also greatly told us the correlation information (fitting slope and R^2) between O_4 DCSDs at 360.8 and 477.1 nm could changes under conditions with different aerosol optical properties. We also added the aerosol information on four different weather conditions in Figure 3 of the manuscript. The measured results and simulation results show good consistency on these four weather conditions of clear periods, light-haze periods, haze periods and heavy-haze periods, especially for heavy-haze periods.

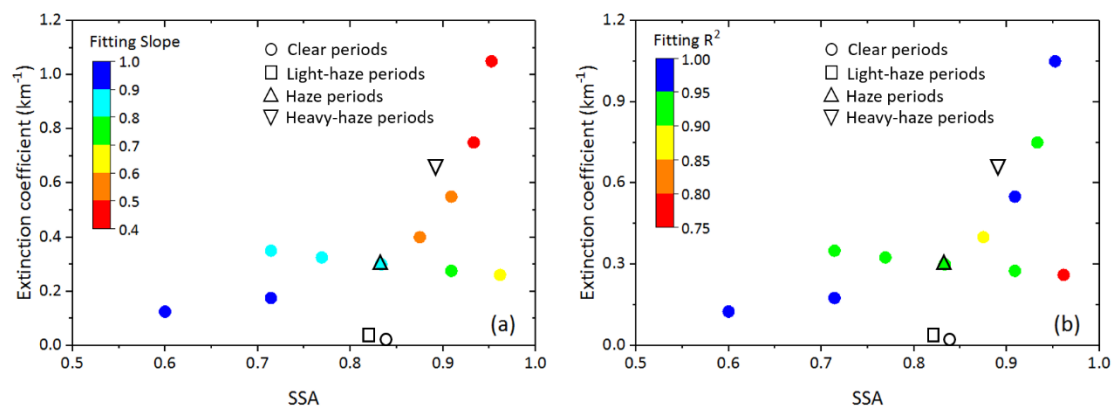


Figure R3. Simulation sensitivity studies of the correlation information (fitting slope and R^2) between O_4 DCSDs at 360.8 and 477.1 nm under conditions with different aerosol optical properties.

(4) P12, Fig.4 => The scat. and abs. changed around 09:05 and 12:00, while the correlation relationship analysis use the break point of 10:00 and 12:00. Why they are different in time? Moreover, why the authors choose the index of variations of scat. instead of abs.?

R: The Figure 4 in the manuscript, we could find the scat. and abs. have lowest values at 09:05 during the time periods of 08:00 to 11:00. However, we have more focused on the change rate (v_{sca} , a_{sca} and a'_{sca} as defined in the manuscript) of scattering and absorption coefficients. The change rate of scattering coefficients (v_{sca} , a_{sca} and a'_{sca}) could be better to help us to understand the relationship the O_4 DSCDs at different wavelength bands and the variations of σ_{sca} and σ_{abs} . For example, the change rate of scattering coefficient at 10:00 is larger than that at 09:05.

We also try to choose the variation of absorption coefficients to identify the break point, but we found it could not identify all the break points as good as the variation

of scattering coefficients. Therefore, we choose the index of variation of scattering coefficients instead of absorption coefficients.

(5) P13-14, Fig.5&6 => The empirical relationships between measured O₄ absorptions in different bands and characteristics of AOPs were mainly concluded from the statistic plot of Fig.5 and Fig.6. I have concerned that the some of the factors (e.g. correlation R² and VIS/UV in haze days, as well as scat. and abs.) have wide value range even cover some cases of other weather conditions. How to obtain the precise and accurate the correspondence between O₄ absorptions and AOPs under different weather conditions?

R: Thanks for your kindly suggestions. As shown in Figure R1 and R3, the fitting slope and R² have different values under conditions with different aerosol optical properties (scattering and absorption coefficient and the corresponding SSA information). Moreover, the corresponding values of O₄ DSCDs in UV and Visible ranges are also different under different conditions. Therefore, it will be a joint decision based on the values of O₄ DSCDs in UV and Visible ranges and the fitting slope and R² between them. This will help us to accurate the correspondence between O₄ absorptions and AOPs.

(6) P16-17, Sect.4 => For the validation, the authors classified the observational period segment into the different weather conditions, however, no further AOPs information, e.g., ADOs, scat. and abs., were inferred and achieved. Is the sentence in line 321(“The σ_{scat} , σ_{abs} and AOD are mainly located at 200-900 Mm⁻¹, 20-60 Mm⁻¹ and 0.9-2.5 under haze and heavy-haze conditions, respectively.”) a conclusion of measurement results or inference from O₄ absorptions?

R: We are very sorry that the description may cause some misunderstanding. The description has been updated as following:

Furthermore, the time series of in-situ σ_{sca} , σ_{abs} and MAX-DOAS retrieved AOD are shown in Fig.7 (c) and (d). According to the empirical relationships summarized above, the σ_{sca} , σ_{abs} and AOD should be mainly located at 200-900 Mm⁻¹, 20-60 Mm⁻¹ and 0.9-2.5 under the haze segment of 09:00-11:00 of 25 November. Simultaneously, the in-situ measured σ_{sca} , σ_{abs} and MAX-DOAS retrieved AOD during the above same periods are ranged in 588.30-730.77 Mm⁻¹, 58.19-67.63 Mm⁻¹ and 1.39-2.22. The inferred results are in good agreement with the measured results. It indicates that the concluded empirical relationships can be used as the criterion to accurately determine the ranges of aerosol optical parameters of σ_{sca} , σ_{abs} and AOD.

We have also supplemented this information in Line 323-329 in the manuscript.

Technical comments

(1) P2, L34: need to be developed

R: Please refer to Line 34.

(2) P2, L83: February of which year?

R: It should be February 2017. Please refer to line 82.

(3) P6, L143: growth => increase

R: Please refer to Line 14-141.

Reference

Frieß, U., Monks, P. S., Remedios, J. J., Rozanov, A., Sinreich, R., Wagner, T., and Platt, U.: MAX-DOAS O₄ measurements: A new technique to derive information on atmospheric aerosols: 2. Modeling studies, *J. Geophys. Res.*, 111, D14203, doi:10.1029/2005JD006618, 2006.

Lee, H., Irie, H., Gu, M., Kim, J., and Hwang, J.: Remote sensing of tropospheric aerosol using UV MAX-DOAS during hazy conditions in winter: Utilization of O₄ Absorption bands at wavelength intervals of 338–368 and 367–393 nm, *Atmospheric Environment*, 45, 5760-5769, 10.1016/j.atmosenv.2011.07.019, 2011.

Wagner, T., Dix, B., von Friedeburg, C., Friess, U., Sanghavi, S., Sinreich, R., and Platt, U.: MAX-DOAS O₄ measurements: A new technique to derive information on atmospheric aerosols—Principles and information content, *J. Geophys. Res.*, 109, D22205, doi:10.1029/2004JD004904, 2004.

Responses to Reviewer #2

First of all, we would like to thank the reviewer for this positive assessment of our manuscript, the constructive and helpful suggestions. Point-to-point responses are given below. The original comments are black in color, while our responses are in blue. All the mentioned line number are referred to the revised manuscript.

Major criticism

(1)The approach to infer aerosol loading condition from the O₄ absorptions is too far from quantitative, although authors mentioned to develop a lookup table to retrieve aerosol optical properties in the future. Aerosol loading information in the level of conditions defined in this study (clear, non-haze, haze, heavy-haze, ect) can be easily told from human eyes. Therefore, the aerosol information inferred from the method of this study has no scientific value.

R: Thanks for your comments. As shown in Figure R1, the retrieval of aerosol extinction coefficients profile from MAX-DOAS measurements is usually performed based on Optimal Estimation Method (OEM) or look-up table method in the previous research (the green box) (Frieß et al., 2016; Beirel et al., 2019). Consequently, the yielded information is the vertical profile of aerosol extinction coefficient without any further specific scattering or absorbing coefficient. However, the research of this manuscript (the red box) is mainly concentrated on the identification of absorption and scattering coefficients directly from the O₄ absorptions with the empirical look-up table, rather than the aerosol loading information. In this way, the a priori information of aerosol for RTM simulation can be avoided, which contains considerable uncertainties in current OEM and look-up method.

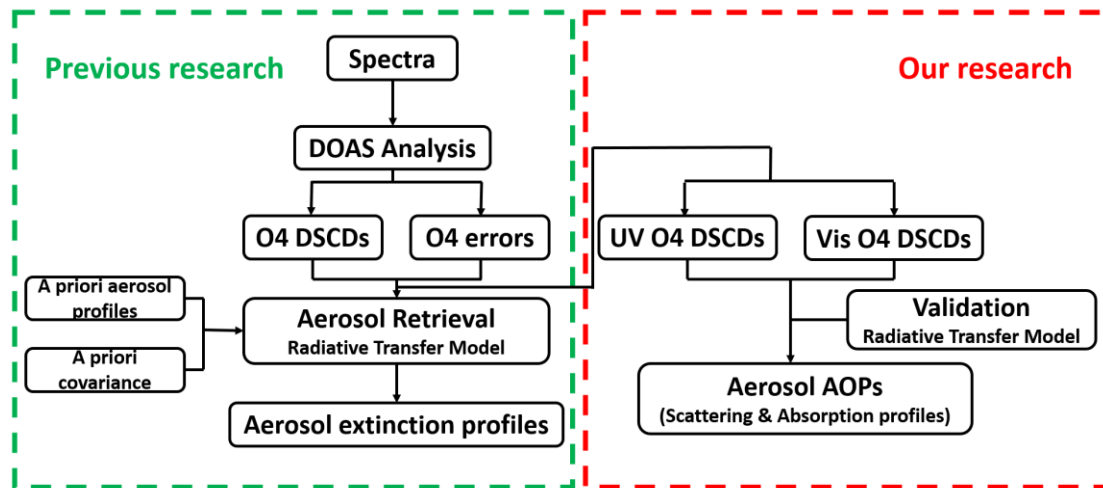


Figure R1. Aerosol profile inversion strategy.

In order to enhance the principle basis of this proposed method, we have used radiative transfer model of SCIATRAN to simulate O₄ DSCDs in UV and Visible bands under conditions with different aerosol optical properties as a validation for the established empirical relationship. As listed in Table 1, 11 different aerosol scenarios were simulated in total, in which case 1 is the default case to represent haze condition. Case 1 to 7 describe the aerosol scenarios of gradually increase of scattering

properties with a fixed σ_{abs} of 0.050 km⁻¹, which cause the growths in both extinction and SSA. Case 8 to 11 present another process of the gradually increase of haze with more absorbing aerosols under the condition that σ_{sca} are fixed on 0.250 km⁻¹, which consequently result in an increase extinction but decrease of SSA.

Table 1. Simulation-based correlation information between O₄ DSCDs at 360.8 and 477.1 nm under conditions with different aerosol optical properties.

	Aerosol information				Slope	R ²	Intercept
	σ_{abs}	σ_{sca}	σ_{ext}	SSA			
1	0.050	0.075	0.125	0.6000	0.9560	0.9968	0.5516
2	0.050	0.125	0.175	0.7143	0.9117	0.9859	0.3178
3	0.050	0.250	0.300	0.8333	0.8089	0.9087	0.1438
4	0.050	0.350	0.400	0.8750	0.5672	0.8842	0.3861
5	0.050	0.500	0.550	0.9091	0.5649	0.9800	0.2305
6	0.050	0.700	0.750	0.9333	0.4519	0.9447	0.2603
7	0.050	1.000	1.050	0.9524	0.4875	0.9979	0.1654
8	0.010	0.250	0.260	0.9615	0.6754	0.7963	0.3948
9	0.025	0.250	0.275	0.9091	0.7682	0.9138	0.2353
10	0.075	0.250	0.325	0.7692	0.8051	0.9007	0.1407
11	0.100	0.250	0.350	0.7143	0.8446	0.9063	0.1011

The linear-regression analysis for the simulated UV and Visible O₄ DSCDs under different aerosol conditions were also listed in Table 1. As shown in Figure R2, the slope and R² between UV and Visible O₄ DSCDs illustrate that:

- (1) Case 1-7 show an exponential trend in Figure R2. The fitting slope decrease accompanied with the increase of extinction coefficients and SSA if the condition of absorption coefficients are determined.
- (2) Case 8-11 show a linear trend in Figure R2. The fitting slope will decrease together with the decrease of extinction coefficients and the increase of SSA when the condition of absorption coefficients are determined.
- (3) The correlation coefficients are high (R² are mainly greater than 0.90) for all the simulation results. As shown in case 8-11, R² decrease accompanied with the decrease of the correlation slopes. This conclusion need to be further supported by more detailed simulations.

We also added the aerosol information on four different weather conditions in Figure R2. The measured results and simulation results show good consistency on these four weather conditions of clear periods, light-haze periods, haze periods and heavy-haze periods, especially for heavy-haze periods.

Finally, it can be expected that the vertical spatial-resolved of aerosol scattering and absorption information can be retrieved by using O₄ DSCDs at different elevation angles, although we could only obtain these information at surface using the O₄ DSCDs at elevation angle 1° now. The accuracy of the determination for aerosol optical properties can be improved when the look-up table is replenished and refined in the future.

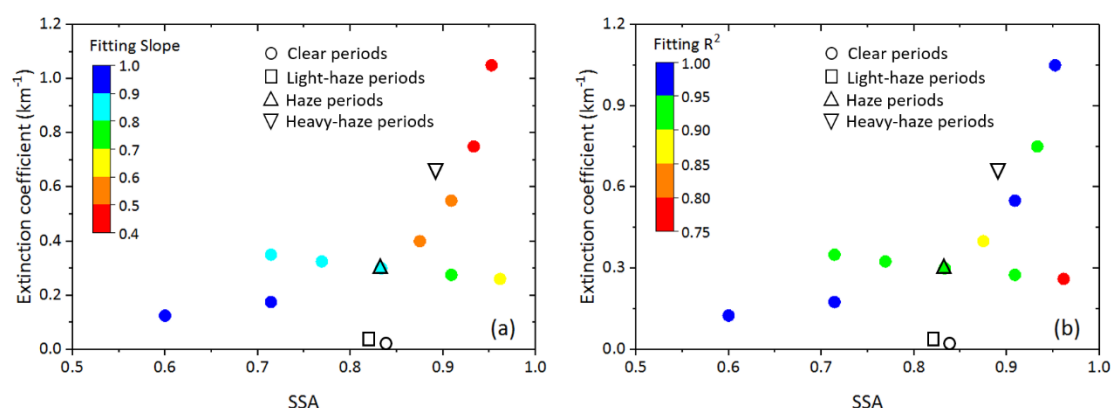


Figure R2. Simulation sensitivity studies of the correlation information (fitting slope and R^2) between O_4 DCSDs at 360.8 and 477.1 nm under conditions with different aerosol optical properties.

(2)Physically, the study methodology is not as much as sound. The O_4 absorption derived from the MAX-DOAS observations are indeed contaminated by aerosols. So in their method, authors intend to use an aerosol-impacted O_4 absorption data to infer the aerosol properties. I think a better way to get information from the MAX-DOAS observation is to retrieve aerosol information (if there is aerosol information) along with the O_4 absorption. Or from another perspective, to study the impact of aerosols to the retrieval accuracy in the O_4 absorption.

R: As shown in Figure R1, the current methodology to retrieve aerosol extinction vertical profile based on MAX-DOAS observed O_4 absorptions is mainly based on the OEM inversion strategy as indicated in the green box of Fig. R1. Considering the uncertainties on the a priori information in the stagey and the single yielded extinction coefficient, our research is aiming to obtain more detailed aerosol optical properties (with absorption and scattering vertical profiles) directly from the O_4 absorptions without the RTM simulation (inversion strategy is described in the red box).

Since the oxygen collision complexes O_4 vertical profile is well known and nearly constant, the observed O_4 absorption can serve as an indicator for the atmospheric distribution of photon paths (Wagner et al., 2004; Frieß et al., 2006). Therefore, the retrieved O_4 differential slant column densities (DSCDs) at different elevations can provide information about the impact of aerosol scattering on photon paths. By combining measurements of the O_4 absorption with radiative transfer model simulations, ground-based MAX-DOAS has been used in previous studies to determine atmospheric aerosol vertical extinction profiles and optical depths (e.g., Irie et al., 2008, 2009; Li et al., 2010; Clémer et al., 2010; Hartl and Wenig, 2013; Hendrick et al., 2014; Vlemmix et al., 2015; Frieß et al., 2016). Moreover, the UV and Visible O_4 DSCDs are used to retrieve aerosol extinction information independently.

In previous, our group have carried out several researches to retrieve aerosol extinction profiles using O_4 DSCDs, which also show the good agreements with external simultaneous measurements, such as Lidar, tethered-balloon observations

(e.g. Xing, et al., 2017; Tan et al., 2018). However, there are still some uncertainties on the retrieval based on Optical Estimation Method (OEM). So we try to establish the new method using O₄ absorptions in UV and Visible ranges to directly get aerosol scattering and absorption information in the study.

(3)I am not convinced with the change speed, acceleration, and the change rate of the acceleration of diurnal scattering coefficient (equations 2-4) for describing the aerosol property change. These variables only make the trivial diurnal analysis more complicated.

R: In order to illustrate the rationality of using the change speed (v_{sca}), acceleration (a_{sca}) and the change rate of acceleration (a'_{sca}) of diurnal scattering coefficients, we selected two examples (February 21 and 11, 2017) to show the evidences.

The example described in Figure R3 is also discussed in the manuscript. We could find the scattering (σ_{sca}) and absorption coefficients (σ_{abs}) have significant variations based on the calculated v_{sca} , a_{sca} and a'_{sca} at ~10:00 and ~12:00, respectively, while the time-indicated O₄ DSCDs seems to be three segments with higher correlation coefficients by the break point of 10:00 and 12:00 (in Figure R3 (a) and (c)).

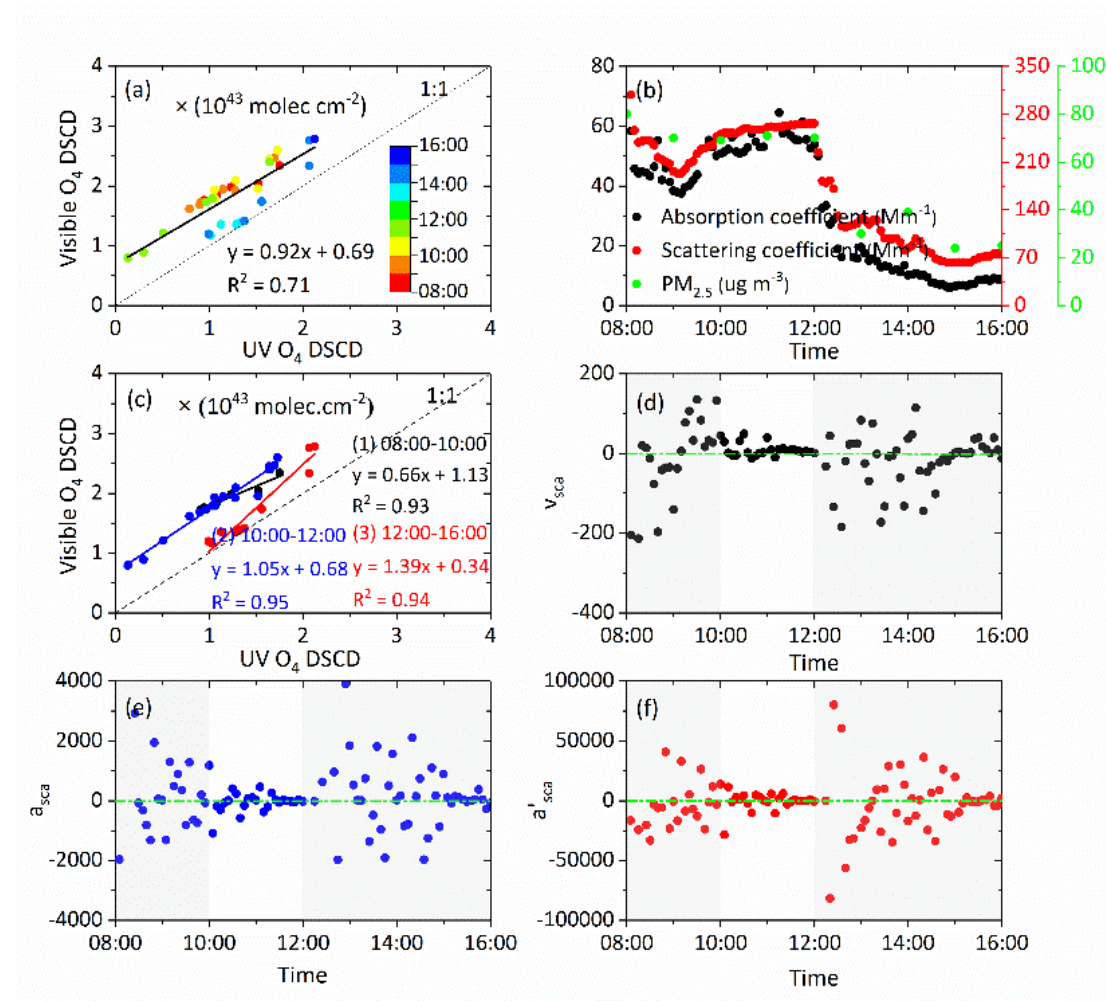


Figure R3. An example day on February 21, 2017: (a) the correlations between O₄ DSCDs

at 360.8 and 477.1 nm. The colorbar represents time sequence. (b) shows the time series of aerosol scattering and absorption coefficients. The correlations information between O_4 DSCDs at 360.8 and 477.1 nm during 08:00-10:00, 10:00-12:00 and 12:00-16:00 were shown in (c). (d) to (f) shows the time series of v_{sca} , a_{sca} and a'_{sca} of scattering coefficients, respectively.

Another case in Figure R4, there are no dramatic changes on σ_{sca} and σ_{abs} during the day. The σ_{sca} decreased slowly in the morning, kept in a stable level during 13:00-15:30, and then increased fast, which presented with three segmental periods (Fig. R4(b)). If we calculated v_{sca} , a_{sca} and a'_{sca} simultaneously, there is only one break point at 15:30 (Fig. R4(d)-(f)). Consequently, the time-indicated O_4 DSCDs of these two segmental periods have higher correlation coefficients. It also indicates aerosol scattering and absorption properties could be mainly manifested in the variations of O_4 absorptions at different wavelength bands.

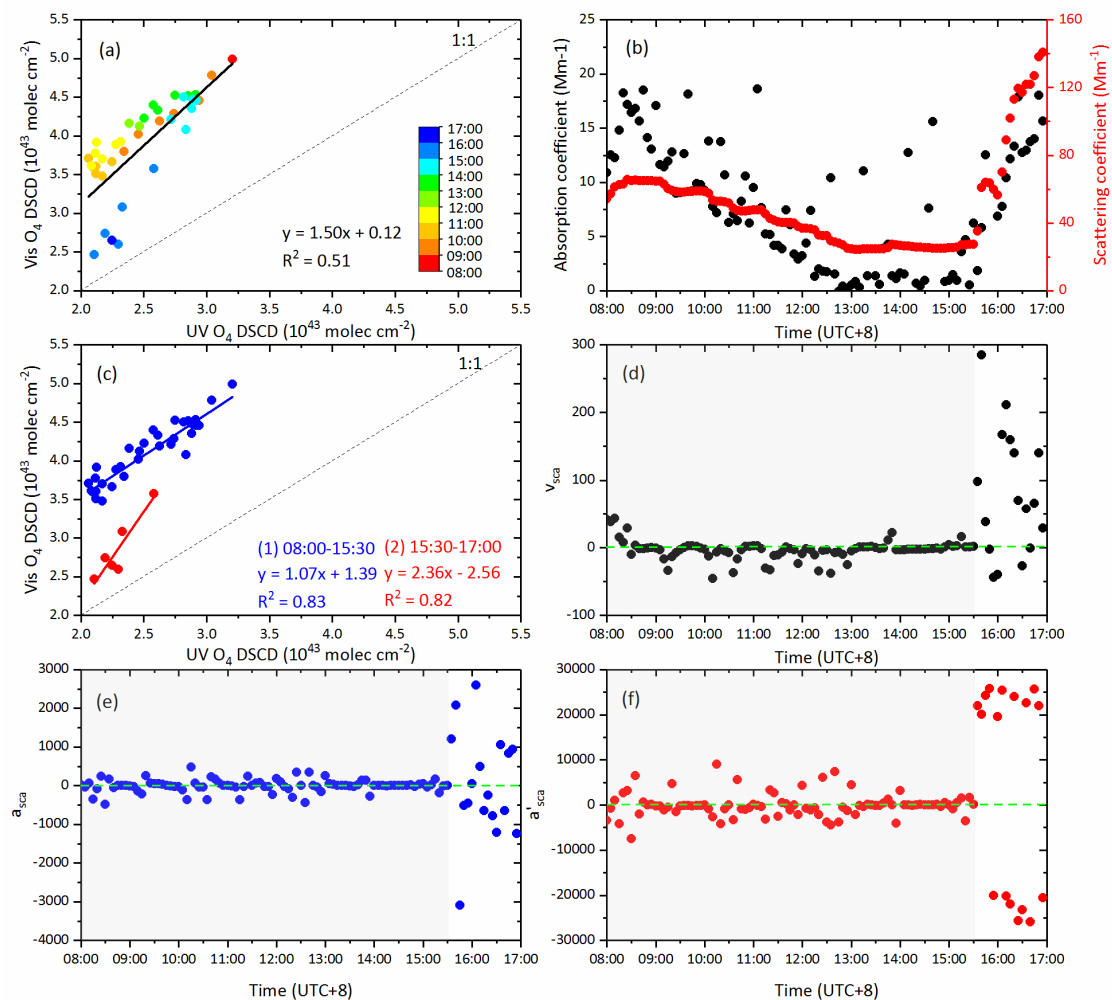


Figure R4. An example day on February 11, 2017: (a) the time series of O_4 DSCDs at 360.8 and 477.1 nm. (b) the correlations between O_4 DSCDs at 360.8 and 477.1 nm. The colorbar represents time sequence. (c) shows the time series of aerosol scattering and absorption coefficients. (d) to (f) shows the time series of v_{sca} , a_{sca} and a'_{sca} of scattering coefficients, respectively.

It can be concluded from Fig. R3 and R4 that the variations on the linear regression analysis between O₄ DSCDs in UV and Visible ranges could better reflect the variations of aerosol scattering and absorption properties. Moreover, the values of O₄ DSCDs are mainly dependent on the light path lengths. It will be difficult to find the break points of scattering coefficients, if we only rely on the values of O₄ DSCDs. Therefore, the above three parameters (change speed, acceleration and the change rate of the acceleration) can help us find the break points of scattering coefficients more accurately, for example in the Fig. R4, the proposed three index can better find the break point than the variation of σ_{sca} itself.

In addition, the calculation of the change speed, acceleration and the change rate of the acceleration are carried out automatically by the coded program, which will not become complicated in practical.

(4)The presentation quality needs improvement. The paper has many grammar issues. I try to catch them in the technical comments below.

R: Thanks for your kindly suggestions. We have improved the presentation quality in the manuscript.

Specific comments

(1)It seems different datasets have different sampling times. It is not clear based on what time length the data are aggregated and compared. Please clarify this.

R: The scattering and absorption coefficient data, the main analytical data, measured at Peking University Urban Atmosphere Environment Monitoring Station (PKUERS, 39.9892°N, 116.3069°E) all have the sampling time of 5 minutes. However, the scattering and absorption data, the data used for validation, measured at Gucheng, Hebei province (39.1382°N, 115.7163°E) have different sampling temporal resolution. The sampling of scattering and absorption coefficient are 1 minute and 1 hour, respectively. We have also clarified in the manuscript. Please refer to line 128 and line 306-307.

(2)Line 160 – 165: the weather conditions are called clear days, ... rainy days. Does it mean that all the data are analysis with on a daily based? If yes, it may be not appropriate, because different weather conditions can happen within a day. If no, these categories should not be called xx days.

R: All the data are analyzed with the hourly averages instead of a daily based. We will change “xx days” to “xx periods”.

(3)I would suggested change “non-haze” into “light-haze”, as “non-haze” means clear. And this condition has an average AOD of 0.35; calling light-haze is more proper.

R: We have corrected them in the whole manuscript according to your suggestion.

(4)Why the elevation angle = 1 degree is chosen for O₄ DSCD used in this study? Please clarify it in the article.

R: Most of scattering and absorption observations were carried out by in-situ instruments at the ground surface. The ground surface aerosol also attracts more attentions due to its closer interactions with ecosystem and human health. Meanwhile, the O_4 absorptions at elevation angle 1° could well reflect the near-surface aerosol information. We only have the in-situ measurements for scattering and absorption coefficients at the ground surface at this moment. Therefore, this study is mainly to focus on the near-surface aerosol optical properties.

Although it is difficult to measure scattering and absorption vertical profiles using in-situ instruments, we are attending to use air ship-based in-situ instruments to measure aerosol scattering and absorption vertical profiles in the near future, which can provide the completed profiles of aerosol scattering, absorption and extinction coefficients. Therefore, we would like further to use O_4 absorptions at multiple different elevation angles to study aerosol scattering and absorption coefficients at different heights. It will also could help us to improve the lookup table.

Technical comments

Line 24: I don't understand the meaning of "O₄ Differential Slant Column Densities (DSCDs) at UV and visible bands varied in the order of ...". Do you mean the magnitude of their correlation coefficients decrease I the order of ...?

R: No, here we mean that the absolute value of O₄ Differential Slant Column Densities (DSCDs) at UV and visible bands all varied "in the order of ...". The DSCDs are usually to denote the absolute value of the results of spectral analysis.

40: aerosols and Aerosol Optical => aerosol loading and Aerosol Optical

40 – 41: Different aerosols behave => Different aerosol types behave

43: heat the air contributing to => heat the air, and contributes to

44: profile causing => profile, causing

R: Please refer to Line 40-44.

48: Please note the AE often refers to Angstrom Exponent.

R: We will use AEC and AE represent Aerosol Extinction Coefficient and Angstrom Exponent in our manuscript, respectively.

49: Angstrom => Angstrom Exponent

51: atmosphere in vertical. => atmosphere.

52: SSA could represent => SSA is defined as

R: Please refer to Line 49-52.

55: the four general aerosol types of biomass burning aerosol, urban-industrial aerosol, dust aerosol and aerosol of marine origin are exhibiting => different aerosol types (such as biomass burning, urban-industrial, dust and sea-salt aerosols) exhibit

R: Please refer to Line 55-56.

63: pronounced SSA => SSA

R: Please refer to Line 61.

71: with maxima at => around

R: Please refer to Line 71.

73: O4 absorptions can be yielded by the DOAS method and further the aerosol vertical profiles at four different wavelength bands (xx). => O4 absorptions in four bands (xx, xx, xx and xx nm) can be estimated, and aerosol vertical profiles can be further derived.

R: Please refer to Line 73-74.

90: Science (CAMS => Science building (CAMS

R: Please refer to Line 89.

95: were used to cover => are used to cover

R: Please refer to Line 94.

93: was equipped with => is equipped with

R: Please refer to Line 96.

106: in UV => in the UV; in visible spectral interval => in the visible

R: Please refer to Line 105.

113: filtered => filtered out; measurements remains for the further discussion. => measurements remained

R: Please refer to Line 111-112.

Table 1: The second line is confusing; No asterisk mark can be found for the table footnote.

R: The asterisk mark at bottom of Table 1 has been removed. We have added the statements about I_0 correction in the text body. Please refer to Line 109-110.

124: several times only during the daytime and only works on non-rainy days => about every 15 minutes during non-rainy daytime.

R: Please refer to 123.

133: Please indicate the distance between Beijing Airport and your site.

R: Please refer to 133.

141: always appeared when PM_{2.5} concentrations increased obviously, and the corresponding AOD also have a significant growth. => coincided with significantly high PM_{2.5} concentration and high AOD.

143: have a significant growth => increases dramatically

R: Please refer to Line 140-141.

143: gray area => gray areas

143: particles pollution => particulate pollution

R: Please refer to Line 142.

150: decreased faster and declined to => decrease sharply to

150: during a shorter while => within a shorter period

R: Please refer to Line 150.

153: are up to => are

154: greater than => over; all the wintertime => the entire wintertime

R: Please refer to Line 153-154.

176: decreased about => decreased by about

R: Please refer to Line 175.

189: at UV => in the UV

R: Please refer to Line 188.

Figure 3: please indicate the time is Beijing Time (UTC+8)

R: We have made the corrections. Please refer to Figure 3 in the revised manuscript.

248: weather types => weather conditions

R: Please refer to Line 250.

255: on the O4 => for the O4

255: at UV band => in the UV band; at visible => in the visible

R: Please refer to Line 257-258.

306: weather type => condition

R: Please refer to Line 310.

325: table. to retrieve => table to retrieve

R: Please refer to Line 332.

330: at UV and visible wavelength bands => in the UV and visible bands

R: Please refer to Line 341.

335: heavy-haze days to. => heavy-haze condition

R: Please refer to Line 346.

341: correlation slope => linear-regression slope

R: Please refer to Line 352.

Reference

Beirle, S., Dörner, S., Donner, S., Remmers, J., Wang, Y., and Wagner, T.: The Mainz profile algorithm (MAPA), *Atmos. Meas. Tech.*, 12, 1785–1806, <https://doi.org/10.5194/amt-12-1785-2019>, 2019.

Clémer, K., Van Roozendaal, M., Fayt, C., Hendrick, F., Hermans, C., Pinardi, G., Spurr, R., Wang, P., and De Mazière, M.: Multiple wavelength retrieval of tropospheric aerosol optical properties from MAXDOAS measurements in Beijing, *Atmos. Meas. Tech.*, 3, 863–878, doi:10.5194/amt-3-863-2010, 2010.

Frieß, U., Monks, P. S., Remedios, J. J., Rozanov, A., Sinreich, R., Wagner, T., and Platt, U.: MAX-DOAS O₄ measurements: A new technique to derive information on atmospheric aerosols: 2. Modeling studies, *J. Geophys. Res.*, 111, D14203, doi:10.1029/2005JD006618, 2006.

Frieß, U., Klein Baltink, H., Beirle, S., Clémer, K., Hendrick, F., Henzing, B., Irie, H., de Leeuw, G., Li, A., Moerman, M. M., van Roozendaal, M., Shaiganfar, R., Wagner, T., Wang, Y., Xie, P., Yilmaz, S., and Zieger, P.: Intercomparison of aerosol extinction profiles retrieved from MAX-DOAS measurements, *Atmos. Meas. Tech.*, 9, 3205–3222, doi:10.5194/amt-9-3205-2016, 2016.

Hartl, A. and Wenig, M. O.: Regularisation model study for the least-squares retrieval of aerosol extinction time series from UV/VIS MAX-DOAS observations for a ground layer profile parameterisation, *Atmos. Meas. Tech.*, 6, 1959–1980, doi:10.5194/amt-6-1959-2013, 2013.

Hendrick, F., Müller, J.-F., Clémer, K., Wang, P., De Mazière, M., Fayt, C., Gielen, C., Hermans, C., Ma, J. Z., Pinardi, G., Stavrou, T., Vlemmix, T., and Van Roozendaal, M.: Four years of ground-based MAX-DOAS observations of HONO and NO₂ in the Beijing area, *Atmos. Chem. Phys.*, 14, 765–781, doi:10.5194/acp-14-765-2014, 2014.

Irie, H., Kanaya, Y., Akimoto, H., Iwabuchi, H., Shimizu, A., and Aoki, K.: First retrieval of tropospheric aerosol profiles using MAX-DOAS and comparison with lidar and sky radiometer measurements, *Atmos. Chem. Phys.*, 8, 341–350, doi:10.5194/acp-8-341-2008, 2008.

Irie, H., Kanaya, Y., Akimoto, H., Iwabuchi, H., Shimizu, A., and Aoki, K.: Dual-wavelength aerosol vertical profile measurements by MAX-DOAS at Tsukuba, Japan, *Atmos. Chem. Phys.*, 9, 2741–2749, doi:10.5194/acp-9-2741-2009, 2009.

Lee, H., Irie, H., Gu, M., Kim, J., and Hwang, J.: Remote sensing of tropospheric aerosol using UV MAX-DOAS during hazy conditions in winter: Utilization of O₄ Absorption bands at wavelength intervals of 338–368 and 367–393 nm, *Atmospheric Environment*, 45, 5760–5769, 10.1016/j.atmosenv.2011.07.019, 2011.

Li, X., Brauers, T., Shao, M., Garland, R. M., Wagner, T., Deutschmann, T., and Wahner, A.: MAX-DOAS measurements in southern China: retrieval of aerosol extinctions and validation using ground-based in-situ data, *Atmos. Chem. Phys.*, 10, 2079–2089, doi:10.5194/acp-10-2079-2010, 2010.

Tan, W., Liu, C., Wang, S., Xing, C., Su, W., Zhang, C., Xia, C., Liu, H., Cai, Z. and Liu, J.: Tropospheric NO₂, SO₂, and HCHO over the East China Sea, using ship-based MAX-DOAS

observations and comparison with OMI and OMPS satellite data, *Atmos. Chem. Phys.*, 18, 15387–15402, <https://doi.org/10.5194/acp-18-15387-2018>, 2018.

Vlemmix, T., Hendrick, F., Pinardi, G., De Smedt, I., Fayt, C., Hermans, C., Pitters, A., Wang, P., Levelt, P., and Van Roozendaal, M.: MAX-DOAS observations of aerosols, formaldehyde and nitrogen dioxide in the Beijing area: comparison of two profile retrieval approaches, *Atmos. Meas. Tech.*, 8, 941–963, doi:10.5194/amt-8-941-2015, 2015.

Wagner T., Dix, B., von Friedeburg, C., Friess, U., Sanghavi, S., Sinreich, R., and Platt, U.: MAX-DOAS O₄ measurements: A new technique to derive information on atmospheric aerosols—Principles and information content, *J. Geophys. Res.*, 109, D22205, doi:10.1029/2004JD004904, 2004.

Xing, C., Liu, C., Wang, S., Chan, K. L., Gao, Y., Huang, X., Su, W., Zhang, C., Dong, Y., Fan, G., Zhang, T., Chen, Z., Hu, Q., Su, H., Xie, Z., and Liu, J.: Observations of the vertical distributions of summertime atmospheric pollutants and the corresponding ozone production in Shanghai, China, *Atmos. Chem. Phys.*, 17, 14275–14289, <https://doi.org/10.5194/acp-17-14275-2017>, 2017.

A new method to determine the aerosol optical properties from multiple wavelength O₄ absorptions by MAX-DOAS observation

Chengzhi Xing¹, Cheng Liu^{1, 2, 3, 7*}, Shanshan Wang^{4, 5*}, Qihou Hu³, Haoran Liu¹, Wei Tan³, Wenqiang Zhang^{3, 6}, Bo Li¹, Jianguo Liu^{2, 3}

¹School of Earth and Space Sciences, University of Science and Technology of China, Hefei, 230026, China

²Center for Excellence in Regional Atmospheric Environment, Institute of Urban Environment, Chinese Academy of Sciences, Xiamen, 361021, China

³Key Lab of Environmental Optics & Technology, Anhui Institute of Optics and Fine Mechanics, Chinese Academy of Sciences, Hefei, 230031, China

⁴Shanghai Key Laboratory of Atmospheric Particle Pollution and Prevention (LAP³), Department of Environmental Science and Engineering, Fudan University, Shanghai, 200433, China

⁵Shanghai Institute of Eco-Chongming (SIEC), No.3663 Northern Zhongshan Road, Shanghai, 200062, China

⁶School of Environmental Science and Optoelectronic Technology, University of Science and Technology of China, Hefei, 230026, China

⁷Anhui Province Key Laboratory of Polar Environment and Global Change, USTC, Hefei, 230026, China

*Correspondence to: Shanshan Wang (shanshanwang@fudan.edu.cn) and Cheng Liu (chliu81@ustc.edu.cn)

Abstract. Ground based Multi-AXis Differential Optical Absorption Spectroscopy (MAX-DOAS) observation was carried out from November 2016 to February 2017 in Beijing, China to measure the O₄ absorptions in UV and visible bands and further to illustrate its relationship with aerosol optical properties (AOPs) under different the weather types. According to relative humidity, visibility and PM_{2.5}, we classified the observation periods into clear, ~~nonlight~~-haze, haze, heavy-haze, fog and rainy five different weather conditions. There are obvious differences for measured AOPs under different weather conditions, especially scattering coefficient (σ_{sca}) and absorption coefficient (σ_{abs}). It was also found that both the O₄ Differential Slant Column Densities (DSCDs) at UV and visible bands varied in the order of clear days > ~~nonlight~~-haze days > haze days > heavy-haze days > fog days. The correlation coefficients (R^2) between O₄ DSCDs at 360.8 and 477.1 nm mainly varied in the order of clear days > ~~nonlight~~-haze days > haze days > heavy-haze days. Based on the statistics of O₄ DSCDs at elevation angle 1° with the corresponding linear regression between UV and visible bands of segmental periods, the relationships between O₄ DSCDs and AOPs were established. It mainly should be clear or ~~nonlight~~-haze days when the correlation slope is greater than 1.0, correlation coefficient (R^2) greater than 0.9 and O₄ DSCDs mainly greater than 2.5×10^{43} molec cm⁻². Meanwhile, σ_{sca} and σ_{abs} are less than 45 and 12 Mm⁻¹, respectively. For haze or heavy-haze days, the correlation slope is less than 0.6, R^2 less than 0.8 and O₄ DSCDs mainly less than 1.3×10^{43} molec cm⁻², under which σ_{sca} and σ_{abs} are mainly located at 200-900 and 20-60 Mm⁻¹. Additionally, the determination method was well validated based on another MAX-DOAS measurement at Gucheng from 19 to 27 November 2016. For more precise and accurate inversion of AOPs, more

detailed look-up tables for O₄ multiple wavelength absorptions need to ~~be~~ developed. Furthermore, the vertical spatial-resolved aerosol scattering and absorption information is worthy of being expected by using DSCDs at different elevation angles.

1 Introduction

Atmospheric aerosols influence the radiative budget by scattering and absorbing solar radiation directly. It also affects the global climate change, cloud formation, regional air quality and human health (Seinfeld and Pandis, 2006; Kim and Ramanathan, 2008; Karanasiou et al., 2012; Levy et al., 2013; Viana et al., 2014). It is important to get a comprehensive knowledge on the spatial distributions, temporal variations of aerosol ~~loadings~~ and Aerosol Optical Properties (AOPs). Different aerosol ~~types~~ behave obviously different optical properties. For example, Black Carbon (BC) aerosols are characterized by the strong light absorption. Recent studies indicated that it can heat the air, ~~and contributes-contributing~~ to global warming (Ramanathan et al., 2007; Galdos et al., 2013; Ramana et al., 2010; Fyfe et al., 2013; Allen et al., 2012). It can also change the atmospheric temperature vertical profile, causing the variations of the planetary boundary layer (PBL) structure (Ding et al., 2016; Wilcox et al., 2016; Wang et al., 2018). However, dust aerosol and some heterogeneous-reaction secondary aerosols, playing an important role during the pollution episode in China, are mainly based on scattering optical characteristics. (Huang et al., 2014; Wang et al., 2018).

Measurements of AOPs, e.g. Aerosol Extinction Coefficient (AEC), Aerosol Optical Depth (AOD), Single Scattering Albedo (SSA), asymmetry factor and Angstrom Exponent, could provide more comprehensive information for a better understanding of the role of aerosols in atmospheric processes. AOD is an important parameter to evaluate the ability of aerosol particles to attenuate the solar radiation, which is defined as the integration of AEC from surface to the top of atmosphere ~~in vertical~~. The AE is the sum of aerosol scattering and absorption coefficients. Moreover, SSA ~~is defined as~~ could present the ratio of scattering efficiency to the total extinction, which is dominant intensive parameter determining aerosols direct radiative forcing. The asymmetric factor is used to evaluate the aerosol forward scattering ability, while the Angstrom is a parameter to evaluate the aerosol particle size. Previous measurements of AOPs indicated that ~~the four general aerosol types of biomass burning aerosol, urban industrial aerosol, dust aerosol and aerosol of marine origin are exhibiting different aerosol types (such as biomass burning, urban-industrial, dust and sea-salt aerosols) exhibit~~ significant differences in optical properties. The differences of the optical properties of these kinds of aerosols are used to clarify the mechanisms of aerosol radiative forcing (Dubovik et al., 2001). For biomass burning aerosol, the Angstrom exponent is mainly distributed between 1.1 and 2.1 at wavelength bands of 440 – 870 nm and SSA mainly ranging from ~0.88 to 0.99 at 440 nm (Eck et al., 2003; Bergstrom et al., 2007; Weinzierl et al., 2017). The SSA of urban-industrial aerosol tend to be ~0.95 in cleaner condition and ~0.85 in industrially condition, respectively (Liousse et al., 1996; Remer and Kaufman, 1998; Garland et al., 2009; He et al., 2009; Shen et al., 2018). Dust exhibits a ~~pronounced~~-SSA ~0.92 to 0.93 in the blue spectral range at 440 nm, but ~0.96 - 0.99 in longer wavelength greater than 550 nm (Kaufman et al., 2001; Dubovik et al., 2001; Bergstrom et al., 2007; Weinzierl et al., 2017). The SSA in oceanic

65 aerosol is mainly greater than 0.97 due to the existing of sea-salt and water soluble particles with high relative humidity (Tanré et al., 1999; Dubovik et al., 2001; Hess et al., 1998; Eck et al., 2005).

Multi-AXis Differential Optical Absorption Spectroscopy (MAX-DOAS) remote sensing is an effective tool for atmospheric aerosol measurements based on O₄ molecular ultraviolet-visible light absorption (Platt and Stutz, 2008). O₄ is the collision complex of O₂ and its concentration is proportional to the square of the O₂ concentration. Due to O₄ vertical profile is well known and nearly constant, it can be served as an indicator for the atmospheric distribution photon paths due to its nearly constant characteristic (Wagner et al., 2004; Frieß et al., 2006; Frieß et al., 2016). The O₄ cross-sections exhibit four main absorption bands in the UV-visible region ~~around with maxima at~~ 360.8, 477.1, 577.1 and 630.8 nm (Thalman and Volkamer, 2013). By collecting the scattered sunlight spectra at zenith and different elevation angles closed to the horizon by MAX-DOAS, the O₄ absorptions ~~in four bands (338-370 nm, 425-490 nm, 540-588 nm and 602-645 nm) can be estimated, and aerosol vertical profiles can be further derived~~ ~~can be yielded by the DOAS method and further the aerosol vertical profiles at four different wavelength bands (338-370 nm, 425-490 nm, 540-588 nm and 602-645 nm)~~ (Honninger and Platt, 2002; Hytch et al., 2003; Hönninger et al., 2004; Wagner et al., 2004; Wittrock et al., 2004; Clémer et al., 2010). The sunlight at different wavelength bands has different ability to traverse the atmosphere, thus the light path length at different wavelength bands are diverse, which can change the corresponding O₄ absorptions. Conversely, the correlation analysis between O₄ absorptions retrieved at UV range and VIS range could also provide information about the impacts of aerosol scattering on photon paths (Lee et al., 2011). Besides the extinction coefficient profile and AOD, there are no detailed researches on the other AOPs retrieval based on MAX-DOAS measurements in previous.

In this paper, we try to establish a new method to determine several different aerosol optical properties from multiple wavelength O₄ absorptions observed by MAX-DOAS measurement. The measurement of UV and visible O₄ absorptions was performed by MAX-DOAS instrument in Beijing from November 2016 to February 2017. Combined the O₄ absorptions and measured AOPs, some empirical relationships between them can be found under different weather conditions, which are the fundamental to determine the AOPs from MAX-DOAS observed O₄ absorptions at different wavelength bands. Furthermore, another short period measurement campaign was used to validate the feasibility and reliability of the new method to infer the AOPs under different weather conditions based on the O₄ absorptions.

90 2 Measurements and methodology

2.1 The MAX-DOAS measurements

The MAX-DOAS instrument was installed on the roof of the Chinese Academy of Meteorological Sciences building (CAMS, 39.9475° N, 116.3273° E) for the continuous measurements of O₄ absorptions from November 2016 to February 2017. The MAX-DOAS instrument consists of three major parts: a telescope unit, two spectrometers with temperature stabilized at 20° and a computer acting as the controlling and data acquisition unit. The viewing elevation angle of the telescope is controlled by a stepping motor. Scattered sunlight collected by the telescope is redirected by a prism reflector and a quartz fibre bundle

to the spectrometers. Two spectrometers (Acton Spectrapro 300i Czerny-Turner optical spectrometer) ~~are were~~ used to cover both the UV (300-460 nm) and visible (400-560 nm) wavelength ranges. The full-width half maximum (FWHM) spectral resolutions of these two spectrometers are all 0.6 nm, or 7.2 detector pixels. Moreover, the optical spectrometer ~~iswas~~ equipped with a CCD detector camera (model DU 440-BU) with 2048 pixels. The field of view (FOV) of the instrument is estimated to be less than 0.5°.

A full measurement scanning sequence consists of eleven elevation angles, i.e., 1, 2, 3, 4, 5, 6, 8, 10, 15, 30 and 90°. The instrument azimuth angle is 138° and the exposure time is fixed to 60000 ms for each elevation angle measurement. A full measurement sequence takes about 11 min. Dark current and offset spectra were measured by blocking incoming light using a mechanical shutter and were subtracted from the measurement spectra before spectral analysis. The routine measurements were continuously repeated as long as the Solar Zenith Angle (SZA) was lower than 80°.

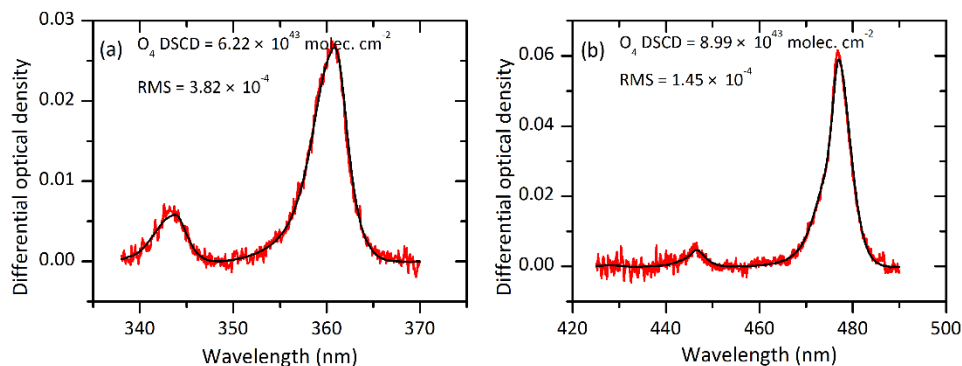
2.2 O4 absorptions in UV and Visible

The O4 absorptions were derived in the fitting windows of 339 to 387 nm in the UV and 425 to 490 nm in the visible spectral interval, respectively. The measured spectra were analysed using the QDOAS software developed by BIRA-IASB (<http://uv-vis.aeronomie.be/software/QDOAS/>). The corresponding zenith spectrum was taken as a reference spectrum for off-zenith elevation angles during each measurement scan. The DOAS fitting generates the Differential Slant Column Density (DSCD) of O4 between the measured spectra and reference spectrum. Details of DOAS fit settings are listed in Table1. We used corrected I0 (Aliwell et al., 2002). Figure 1 shows a typical DOAS retrieval for the O4 absorptions at 360.8 and 477.1 nm. Afterwards, DOAS fit results with a root mean square (RMS) larger than 5×10⁻⁴ were filtered out, and about 99.07% of all O4 measurements ~~remained~~remains for the further discussion.

Table 1. DOAS retrieval settings for O4.

Parameter	Data source	O4 Fitting intervals	
Wavelength range		338-370 nm	425-490 nm
NO2	298K, I0-corrected, Vandaele et al. (1998)	√	√
NO2	220K, I0-corrected, Vandaele et al. (1998)	×	√
O3	223K, I0-corrected, Serdyuchenko et al. (2014)	√	√
O3	243K, I0-corrected, Serdyuchenko et al. (2014)	√	×
O4	293K, Thalman and Volkamer (2013)	√	√
HCHO	298K, Meller and Moortgat (2000)	√	×
H2O	HITEMP (Rothman et al. 2010)	×	√
BrO	223K, Fleischmann et al. (2004)	√	×
Ring	Calculated with QDOAS	√	√
Polynomial degree		Order 5	Order 4
Intensity offset		Constant	Constant

*Solar I0 correction, Aliwell et al., 2002



120 **Figure 1. Typical DOAS spectral fittings for O₄ absorptions in (a) UV and (b) visible bands. Black lines represent the absorption signal and the red lines represent the sum of the absorption signal and the fit residual.**

2.3 Ancillary data

Quality-assured Level 2.0 sunphotometer AODs, Asymmetric factor and Angstrom at the Beijing_CAMS AERONET site
 125 (<http://aeronet.gsfc.nasa.gov/>) were employed, which is collocated with the MAX-DOAS instrument just 2 meters nearby. Sunphotometer (CE-318) collects direct sunlight ~~about every 15 minutes during non-rainy daytime, several times only during the daytime and only works on non-rainy days~~. These aerosol optical parameters at multiple wavelengths were normalized to 450 nm according to Wang et al. (2016). Besides, the scattering coefficients (σ_{sca}) were measured at three wavelength ($\lambda = 450, 520$ and 700 nm) using an integrating nephelometer (Aurora 4000, Ecotech) at Peking University Urban Atmosphere
 130 Environment Monitoring Station (PKUERS, 39.9892° N, 116.3069° E). The absorption coefficients (σ_{abs}) were measured using a 7-wavelength Aethalometer (AE-31, Magee Scientific) at $\lambda = 370, 470, 520, 660, 880$ and 950 nm also located at PKUERS. ~~Both σ_{sca} and σ_{abs} have the sampling temporal resolution of 5 minutes.~~ In order to ensure the accuracy of the data, the corrections for σ_{sca} and σ_{abs} were referred to Shen et al. (2018). The SSA was calculated by the measured σ_{sca} at 450 nm and estimated σ_{abs} at 450 nm using the following equation:

$$135 \quad \text{SSA} = \frac{\sigma_{\text{sca}}}{\sigma_{\text{sca}} + \sigma_{\text{abs}}} \quad (1)$$

The visibility and the relative humidity (RH) information were collected from the weather history data at Beijing international airport (<http://www.wunderground.com/>) ~~about 26 km from CAMS~~. In-situ data of PM_{2.5} concentrations were obtained from Guanyuan station (39.9425° N, 116.3610° E), belonging to the national environmental monitoring network (<http://beijingair.sinaapp.com/data/china/sites/>), which is about ~ 2 km from the CAMS site. All these data are normalized to
 140 hourly averages for further discussion.

3 Results

3.1 Wintertime aerosols optical properties

The time series of PM_{2.5} concentrations, σ_{sca} , σ_{abs} , SSA, AOD, Angstrom, asymmetry factor and the corresponding meteorological data, i.e. RH and visibility, from November 2016 to February 2017 are presented in Fig. 2. The typical meteorological conditions of high RH and low visibility ~~always appeared when PM_{2.5} concentrations increased obviously, and the corresponding AOD also have a significant growth~~ coincided with significantly high PM_{2.5} concentration and high AOD. As indicated in the gray areas of Fig. 2, two episodes of ~~particulate particles~~ pollution during 15 to 22 December 2016, and 29 December 2016 to 2 January 2017 were identified.

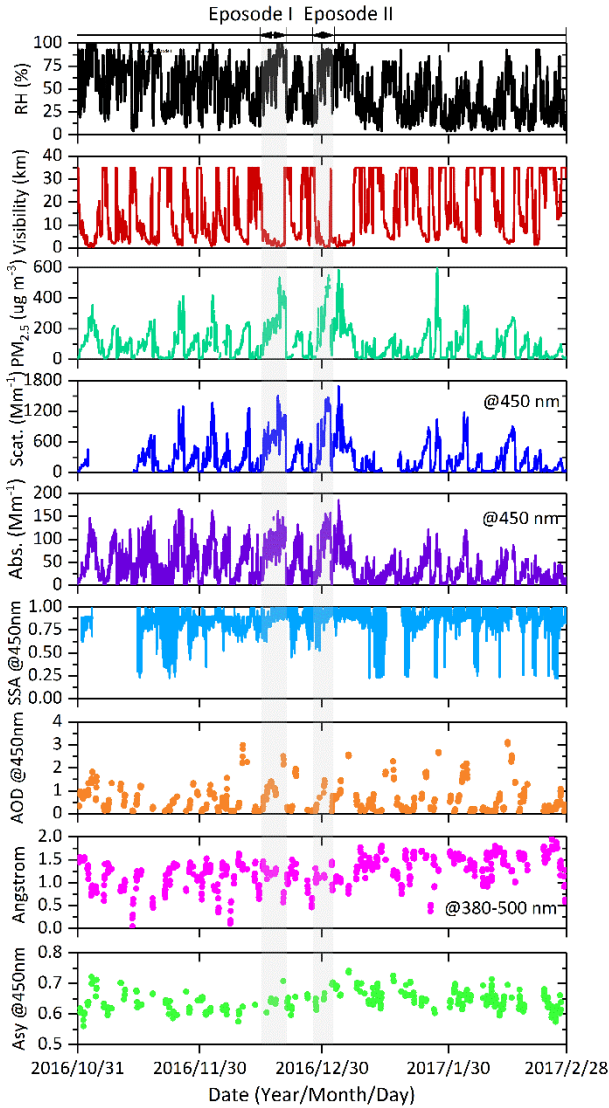


Figure 2. Time series of PM_{2.5} and AOPs (σ_{sca} , σ_{abs} , SSA, AOD, Angstrom and Asymmetry factor), and meteorological parameters (relative humidity and visibility) during the observation in Beijing from November 2016 to February 2017.

During these two episodes, PM_{2.5} concentrations, σ_{sca} and σ_{abs} typically increased and remained in a high level for several days, however, ~~decrease sharply decreased faster and declined~~ to a lower value ~~within during~~ a shorter ~~period~~while. PM_{2.5} concentrations, σ_{sca} and σ_{abs} increased to exceeding the maximum values 465 $\mu\text{g cm}^{-3}$, 1331.151 Mm^{-1} and 123.402 Mm^{-1} within 1-3 hours (the increment up to 200 $\mu\text{g cm}^{-3}$, 600 Mm^{-1} and 100 Mm^{-1}) during episode I, respectively. In episode II, the maximum values of PM_{2.5} concentrations, σ_{sca} and σ_{abs} are ~~up to~~ 585 $\mu\text{g cm}^{-3}$, 1473.523 Mm^{-1} and 153.431 Mm^{-1} , respectively. In addition, SSA mainly kept ~~greater than over~~ 0.85 during ~~the entire all the~~ wintertime, except it was observed to be less than 0.8 in late November 2016 and several days during January and February 2017. Generally, the high values of SSA were always accompanied by the peak of PM_{2.5} concentrations, which suggests that the scattering properties of atmospheric aerosols were enhanced during the explosive increase stage of particles concentrations. Meanwhile, it is also associated with the decreasing of Angstrom and the increasing of asymmetry factors simultaneously. This is typically related to the particle size growth process (Guo et al., 2014; Yu et al., 2011; Yu et al., 2016).

In order to investigate the AOPs under different weather conditions, we classified observation periods of these four months into six scenarios according to the RH, visibility and PM_{2.5} concentration: Clear days (Visibility > 20 km & PM_{2.5} ≤ 35 $\mu\text{g m}^{-3}$ & RH < 80%), ~~NonLight~~-haze days (10 km < Visibility ≤ 20 km & 35 $\mu\text{g m}^{-3}$ < PM_{2.5} ≤ 75 $\mu\text{g m}^{-3}$ & RH < 80%), Haze days (RH ≤ 80% & 5 km < Visibility ≤ 10 km & 75 $\mu\text{g m}^{-3}$ < PM_{2.5} ≤ 115 $\mu\text{g m}^{-3}$), Heavy-haze days (RH ≤ 80% & Visibility ≤ 5 km & PM_{2.5} > 115 $\mu\text{g m}^{-3}$), Fog days (RH > 80% & Visibility ≤ 5 km) and Rainy days (Zheng et al., 2015; Duan et al., 2016). As expected, the AOPs showed distinct characteristics during these different weather conditions. Table 2 summarizes the statistics of Air Quality Index (AQI) and AOPs under the six scenarios. AQI is factor to comprehensively evaluate the air quality, which is based on six pollutants of ambient O₃, NO₂, CO, SO₂, PM₁₀ and PM_{2.5}.

With the increasing of pollution level indicated by AQI (except fog and rainy days), AOD increased dramatically from 0.311 under clear days to 1.338 in heavy-haze days. There are no obvious changes for σ_{sca} and σ_{abs} between clear days and ~~nonlight~~-haze days. Nevertheless, the σ_{sca} increased sharply from ~~nonlight~~-haze days to heavy-haze days with the averaged value from 44.524 Mm^{-1} to 449.741 Mm^{-1} . The averaged value of σ_{abs} is 8.257 Mm^{-1} in ~~nonlight~~-haze days and it increased as much as 5 times in heavy-haze days. Moreover, the averaged SSA was about 0.847 on ~~nonlight~~-haze days and similar to that in haze days, but it increased about 3.53% from haze days to heavy-haze days with the averaged values from 0.846 to 0.878. It suggests that the aerosol scattering and absorption abilities have changed evidently but the ratio of scattering to extinction have changed slightly during the processes of particle pollution became severe. No obvious variations on Angstrom were observed among clear days to heavy-haze days, but it decreased ~~by~~ about 2.83% in fog days. In previous study, the Angstrom are usually higher than 0.80 when AOD is greater than 0.60 in Beijing, which reveals the major contribution of small particles for higher aerosol loading (Che et al., 2015). However, our study demonstrates that small particles made a major contribution to the aerosols

throughout the whole wintertime in Beijing. The obvious decrease of Angstrom in fog days is attributed to the increase of
185 water vapour in particles. In addition, the averaged asymmetry factor was about 0.697 in fog days and 8.52% higher than other
weather conditions. It indicates the increased forward scattering in fog days (Yoon and Kim, 2006).

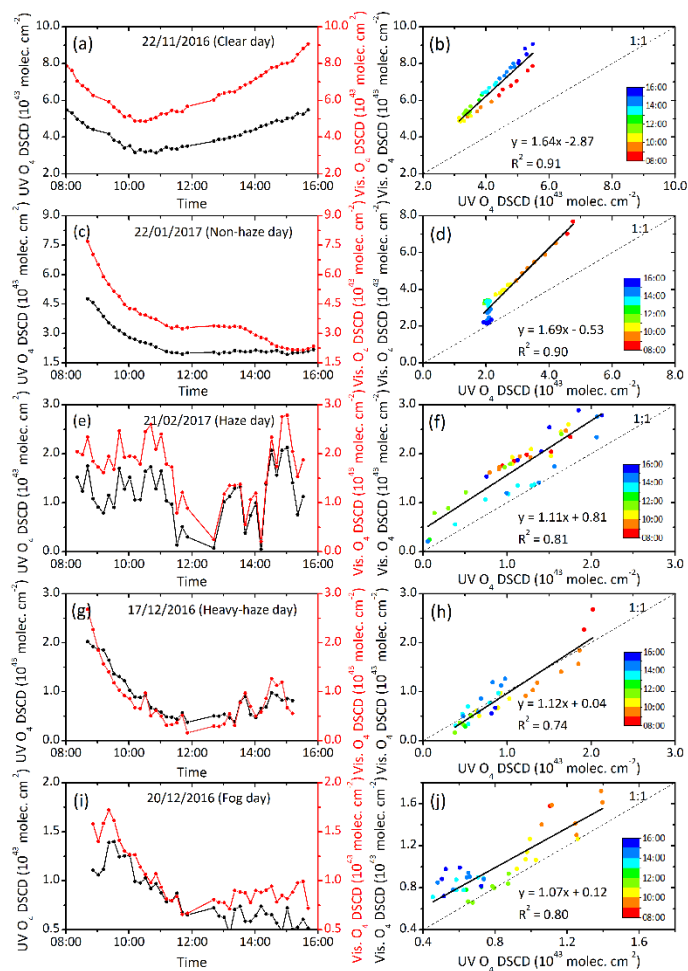
Table 2. Statistics of AQI and several aerosol optical properties under different weather conditions.

Weather condition AQI and AOPs	Clear day			NonLight-haze day			Haze day			Heavy-haze day			Fog day			Rainy day		
	Visibility > 20 km & PM _{2.5} ≤ 35 ug m ⁻³ & RH < 80%			10 km < Visibility ≤ 20 km & 35 ug m ⁻³ < PM _{2.5} ≤ 75 ug m ⁻³ & RH < 80%			5 km < Visibility ≤ 10 km & 75 ug m ⁻³ < PM _{2.5} ≤ 115 ug m ⁻³ & RH ≤≤ 80%			Visibility ≤ 5 km & PM _{2.5} > 115 ug m ⁻³ & RH ≤≤ 80%			Visibility ≤ 5 km & RH > 80%			RH > 80%		
	Ave.	min	max	Ave.	min	max	Ave.	min	max	Ave.	min	max	Ave.	min	max	Ave.	min	max
AQI	24	5	44	60	15	119	130	39	391	214	43	500	306	26	500	106	15	500
σ _{abs}	7.356	0.605	63.999	8.257	1.003	37.229	39.985	2.142	103.421	53.257	3.322	105.290	89.625	7.634	156.878	28.137	2.296	94.639
σ _{sca}	41.411	3.920	214.581	44.524	8.889	305.853	259.081	5.872	809.550	449.741	14.093	1096.859	739.152	53.895	1662.896	217.125	25.938	656.143
SSA	0.854	0.419	0.975	0.847	0.518	0.953	0.846	0.438	0.931	0.878	0.686	0.930	0.887	0.790	0.928	0.878	0.764	0.941
Asy	0.640	0.560	0.714	0.643	0.599	0.670	0.639	0.575	0.704	0.647	0.598	0.742	0.697	0.660	0.708			
Angstrom	1.252	0.210	1.943	1.304	0.429	1.950	1.265	0.176	1.853	1.286	0.798	1.731	1.054	0.568	1.759			
AOD	0.311	0.051	0.799	0.351	0.103	0.927	0.892	0.645	2.495	1.338	0.939	2.693	0.998	0.105	2.509			

3.2 UV and visible O₄ absorptions under different weather conditions

Figure. 3 shows the examples of diurnal pattern and corresponding correlation of UV and visible O₄ DSCDs (elevation angle = 1°) at 360.8 and 477.1 nm under five different weather conditions, except for the rainy days. In view of the absolute strength of O₄ absorption, both the O₄ DSCDs ~~in the~~ UV and visible bands varied in the order of clear days > ~~nonlight~~-haze days > haze days > heavy-haze days > fog days. It manifested the dependency of O₄ absorption on the scattering sunlight path impacted by the aerosol loading. Moreover, O₄ DSCDs at 477.1 nm are obviously higher than that at 360.8 nm in clear and ~~nonlight~~-haze days, and slightly larger than that at 360.8 nm in haze and heavy-haze days, which can be explained by the fact that the observable light path length at visible range is longer than UV range. Even in UV bands, the observed O₄ DSCDs at 353 nm were reported to be lower than those at 380 nm for most of the elevations under haze conditions during winter in Beijing (Lee et al. 2011). This phenomenon revealed that O₄ absorptions in short wavelength range were more significantly affected by light diffusion under hazy conditions. However, we found there is no obvious differences between O₄ DSCDs at 360.8 and 477.1 nm in fog days, during which the high contents of water vapour decreased the visibility and the atmospheric absorption paths from UV to visible range.

We further analysed the relationship of O₄ absorptions between UV and visible bands. As shown in the right column of Fig. 3, the correlation coefficient (R²) of O₄ DSCDs between at 360.8 and 477.1 nm varied in the order of clear days > ~~nonlight~~-haze days > haze days > heavy-haze days. Strong correlation between UV and visible O₄ absorptions (R² > 0.9) was achieved for clear and ~~nonlight~~-haze days. Under haze and heavy-haze conditions, R² was 0.81 and 0.74, respectively, which are much lower than that in clear and ~~nonlight~~-haze days. That is because the increase of light-absorbing and light-scattering aerosols can result in reduced light path lengths more obviously in shorter wavelength bands than longer wavelength bands during haze and heavy-haze days.



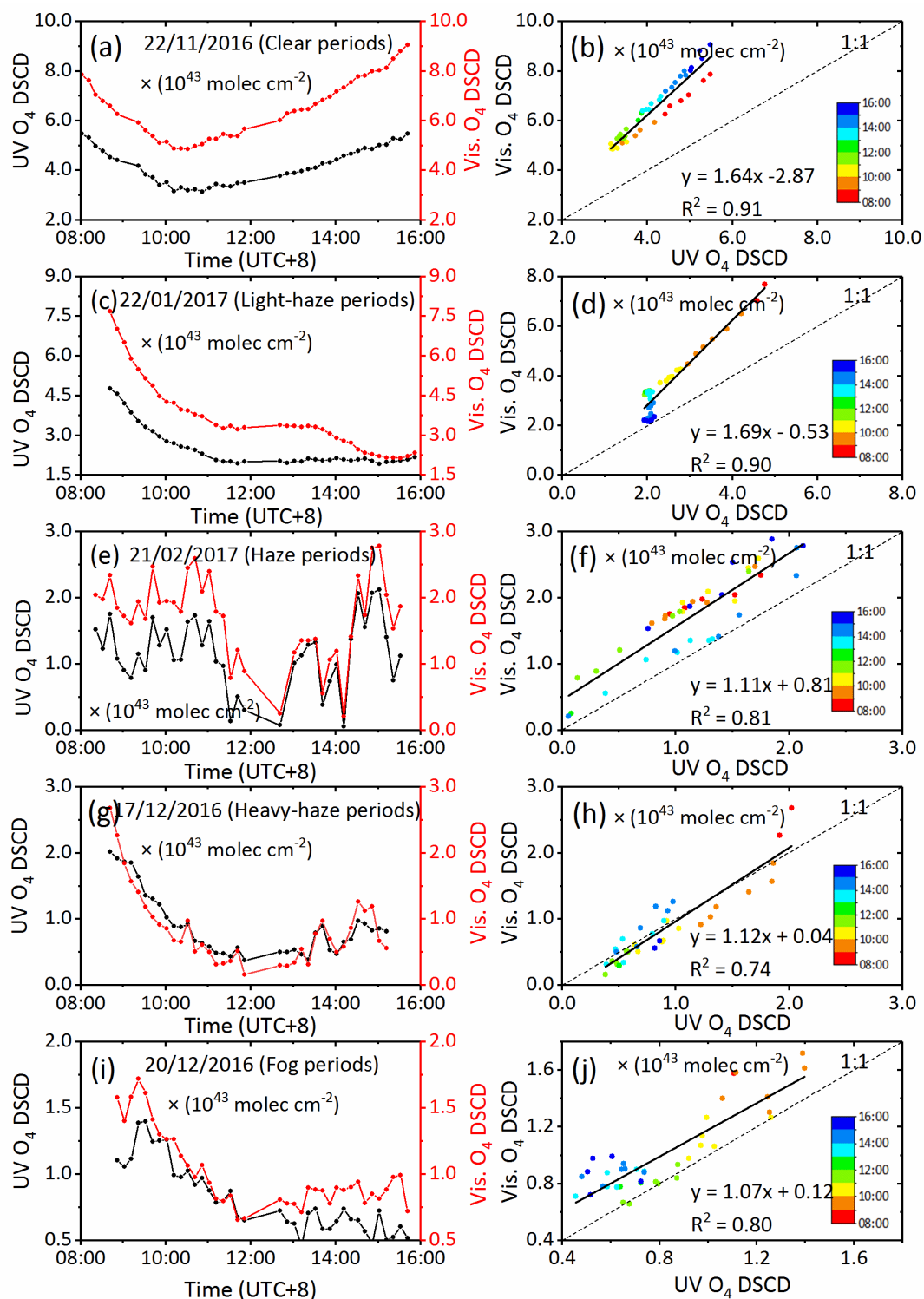


Figure 3. Diurnal variation and correlation analysis of O₄ DSCDs at 360.8 and 477.1 nm under different weather conditions: (a) and (b) clear day, (c) and (d) nonlight-haze day, (e) and (f) haze day, (g) and (h) heavy-haze day, (i) and (j) fog day. The colorbar represents the time sequence.

The changes of AOPs, especially aerosol scattering and absorption properties, are mainly manifested in the variations of O₄ absorptions at different wavelength bands. The correlation information of O₄ DSCDs at different bands will also be affected by the variation of AOPs. For more detailed, i.e., 21 February 2017, was chosen to exhibit the influence of AOPs changes on O₄ DSCDs in Fig. 4. Compared Fig. 4 (a) to (b), it can be found that σ_{sca} and σ_{abs} have a similar variation trends, a slightly turning and an abruptly decrease occurred at ~09:05 and ~12:00 (especially for σ_{sca}), respectively, while the time-indicated O₄ DSCDs seems to be three segments with higher correlation coefficient divided by the break point of 10:00 and 12:00.

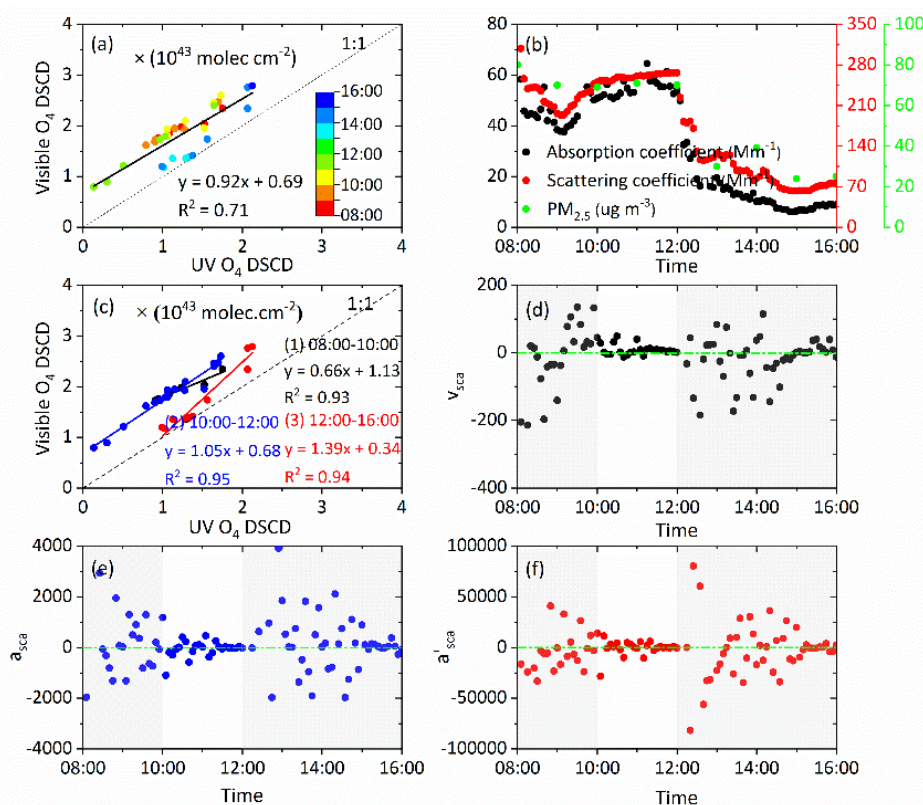


Figure 4. An example day on 21 February 2017: (a) the correlations between O₄ DSCDs at 360.8 and 477.1 nm. The colorbar represents time sequence. (b) shows the time series of aerosol scattering and absorption coefficients. The correlations information between O₄ DSCDs at 360.8 and 477.1 nm on 08:00-10:00, 10:00-12:00 and 12:00-16:00 21 February 2017 were shown in (c). (d) to (f) shows the time series of v_{sca} , a_{sca} and a'_{sca} of scattering coefficients, respectively.

In order to explore the relationship between the O₄ DSCDs at different wavelength bands and the variations of σ_{sca} and σ_{abs} , we defined the change speed (v_{sca}), acceleration (a_{sca}) and the change rate of acceleration (a'_{sca}) of σ_{sca} (Fig4 (b), (e) and (f)) as the following three equations,

$$v_{\text{sca}} = \frac{d\sigma_{\text{sca}}}{dt} \quad (2)$$

$$a_{\text{sca}} = \frac{dv_{\text{sca}}}{dt} \quad (3)$$

$$a'_{\text{sca}} = \frac{da_{\text{sca}}}{dt} \quad (4)$$

Accordingly, the relevant time series of v_{sca} , a_{sca} and a'_{sca} are displayed in Fig. 4 (d) to (f). In this case, we can find two time break points, defined as t_1 and t_2 ($t_1 = 10:00$ and $t_2 = 12:00$), at which σ_{sca} and σ_{abs} have significant variations based on the calculated v_{sca} , a_{sca} and a'_{sca} . In addition, we found the indicator of a'_{sca} can describe the specific moment at which the change (increasing or decreasing) of σ_{sca} more clearly than v_{sca} and a_{sca} in this case. $|a'_{\text{sca}1}|$ and $|a'_{\text{sca}2}|$ are all higher than 20000. Consequently, the O₄ DSCDs at 360.8 and 477.1 nm can be divided into three segments for the periods of 08:00-10:00, 10:00-12:00 and 12:00-16:00 and the correlation between UV and VIS O₄ DSCDs was further analysed individually. As shown in Fig. 4(c), the R^2 during 08:00-10:00 and 10:00-12:00 is obviously larger than that of all day in Fig. 4(a), however, it is smaller for segment of 12:00-16:00. Moreover, there were huge divergences among the correlation slopes among these three segments due to the change of aerosol scattering and absorption properties. Therefore, it can be concluded that the diurnal variations of O₄ DSCDs provide the information of the light path length impacted by aerosol loading, and further the varied relationship between O₄ DSCDs at UV and visible implies the change of the aerosol scattering and absorption properties.

Using the method discussed above, we have defined the time break points with aerosol properties changes and further classified the observation into several segmental periods with the criterion of $|v_{\text{sca}}| > 1000$ or $|a_{\text{sca}}| > 10000$ or $|a'_{\text{sca}}| > 20000$. The summary of time break points and corresponding change speed (v_{sca}), acceleration (a_{sca}) and the change rate of acceleration (a'_{sca}) of σ_{sca} were listed in Table S1.

3. 3 Implications of O₄ absorptions to aerosol optical properties

In order to derive the aerosol optical properties from multiple wavelength O₄ absorptions, the complete four months observational O₄ and AOPs data were used for discussion under different weather conditiontypes. Hourly data of O₄ DSCDs were divided into five weather conditions and made the linear regression between UV and VIS O₄ DSCDs. In total, there were about 218 segments (776 hours in 97 days), including 67, 31, 61, 44 and 15 segments for clear, nonlight-haze, haze, heavy-haze and fog days, respectively. Figure 5 illustrated the statistics of O₄ DSCDs in UV and visible bands, and the slope and R^2 of correlation analysis between them, as well as the O₄ DSCDs ratio of UV to visible for different weather conditions.

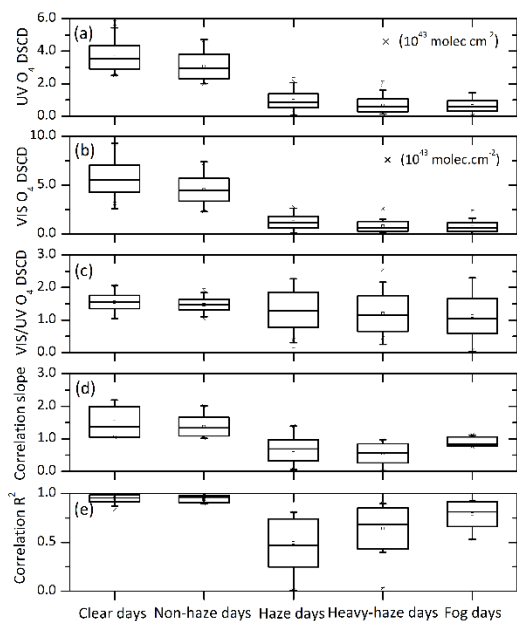


Figure 5. Box plots of statistics for on the O₄ DSCD under different weather conditions: (a) in the ~~at~~-UV band, (b) In the ~~at~~-visible band, (c) the ratio of VIS/UV O₄ DSCD, (d) correlation slope and (e) R² between UV and visible (Visible O₄ DSCD=slope*UV O₄ DSCD + intercept).

In general, the O₄ DSCDs in UV are mainly ranged in $3.00-4.00 \times 10^{43}$, $2.50-3.50 \times 10^{43}$, $0.50-1.10 \times 10^{43}$, $0.25-0.80 \times 10^{43}$ and $0.20-0.40 \times 10^{43}$ molec cm⁻² in clear, ~~nonlight~~-haze, haze, heavy-haze and fog days, respectively. And the O₄ DSCDs in visible are mainly distributed between $4.00-6.50 \times 10^{43}$, $3.00-5.50 \times 10^{43}$, $0.50-1.30 \times 10^{43}$, $0.25-0.60 \times 10^{43}$ and $0.25-0.60 \times 10^{43}$ molec cm⁻² under above five different weather conditions, which are higher than those in UV especially for clear and ~~nonlight~~-haze days. Moreover, the corresponding ratio of visible to UV O₄ DSCDs are 1.45-1.70, 1.45-1.65, 1.00-1.65, 0.85-1.35 and 0.80-1.35 under these five weather conditions, respectively. The linear regression results show that the correlation slopes between UV and visible O₄ DSCDs are greater than 1.00 (mainly greater than 1.40) and the correlation R² are greater than 0.93 mostly in clear days. Under ~~nonlight~~-haze condition, the correlation slopes are greater than 1.00 (mainly greater than 1.20) and the correlation R² are mainly greater than 0.90, respectively. The correlation slopes are mainly less than 0.60 and the correlation R² have a wider range (the maximum value < 0.80 and occasional fitting failure) in haze days. In heavy-haze days, the correlation slopes are less than 0.60-0.80 and the correlation R² are 0.50-0.80 mostly (some fitting failure cases appeared). In fog days, the correlation slopes are floated around 1.00 and the correlation R² are mainly 0.75-0.85, respectively.

Meanwhile, the statistical characteristics of AOPs under different weather conditions are shown in Fig. 6. Similar to the results in Table 2, σ_{sca} shows the increasing trend and were mainly distributed between 21.83-47.01, 28.33-57.25, 134.72-349.47, 228.42-649.11 and 450.00-1004.88 Mm⁻¹ in clear, ~~nonlight~~-haze, haze, heavy-haze and fog days, respectively. The σ_{abs} were mainly distributed between 2.61-8.26, 3.99-11.89, 22.25-57.31, 34.84-72.22 and 70.01-115.26 Mm⁻¹ under above five different

weather conditions. The AODs were mainly distributed between 0.11-0.35, 0.12-0.37, 0.76-1.70, 1.37-2.38 and 0.69-1.38 under these five weather conditions. The Angstrom were more disperse for clear and ~~nonlight~~-haze days than the other weather conditions. Except the fog days, the asymmetry factor in other weather conditions are not much different.

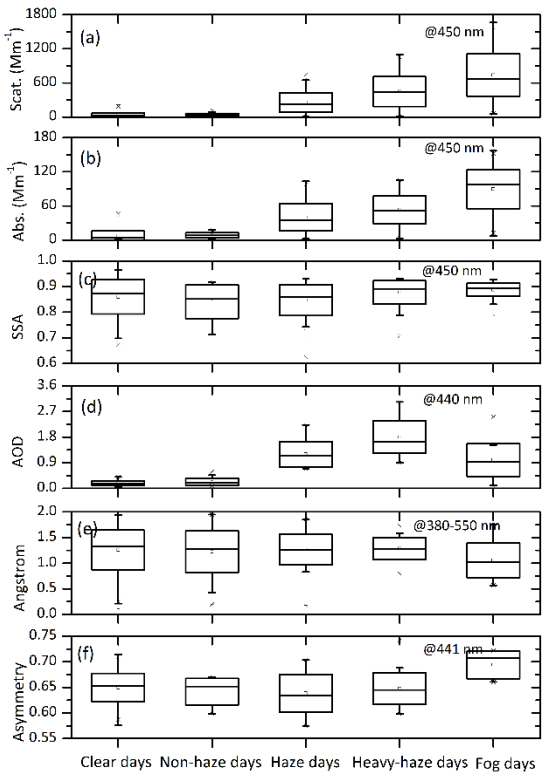


Figure 6. Box plots of the statistics on aerosol optical properties under different weather conditions: (a) σ_{sca} , (b) σ_{abs} , (c) SSA, (d) AOD, (e) Angstrom and (f) Asymmetry.

290 Combined the statistical information on O₄ absorptions and AOPs, we could conclude some empirical relationships as following:

- 295
- (1) Under the condition that the correlation slopes between UV and visible O₄ DSCDs greater than 1.0 and the correlation R² greater than 0.9, simultaneously, the UV and visible O₄ DSCDs are mainly greater than 2.5×10^{43} molec cm⁻² and 3.0×10^{43} molec cm⁻², we could know the weather mainly should be clear or ~~nonlight~~-haze days. It can be suspected that σ_{sca} and σ_{abs} are less than 45 Mm⁻¹ and 12 Mm⁻¹, and AODs are less than 0.4.
 - (2) Under the condition of the correlation slope less than 0.6 and the correlation R² less than 0.8, simultaneously, the UV and visible O₄ DSCDs are mainly less than 1.1×10^{43} molec cm⁻² and 1.3×10^{43} molec cm⁻², the weather mainly should be haze or heavy-haze days. Moreover, σ_{sca} and σ_{abs} are estimated to be distributed at 200-900 Mm⁻¹ and 20-60 Mm⁻¹,

respectively. AODs are between 0.9 and 2.5. In more detail, σ_{sca} , σ_{abs} and AOD will be located at 200-400 Mm^{-1} , 20-50 Mm^{-1} and 0.9-1.5 under the condition of UV and visible O_4 DSCDs $> 1.0 \times 10^{43} \text{ molec.cm}^{-2}$.

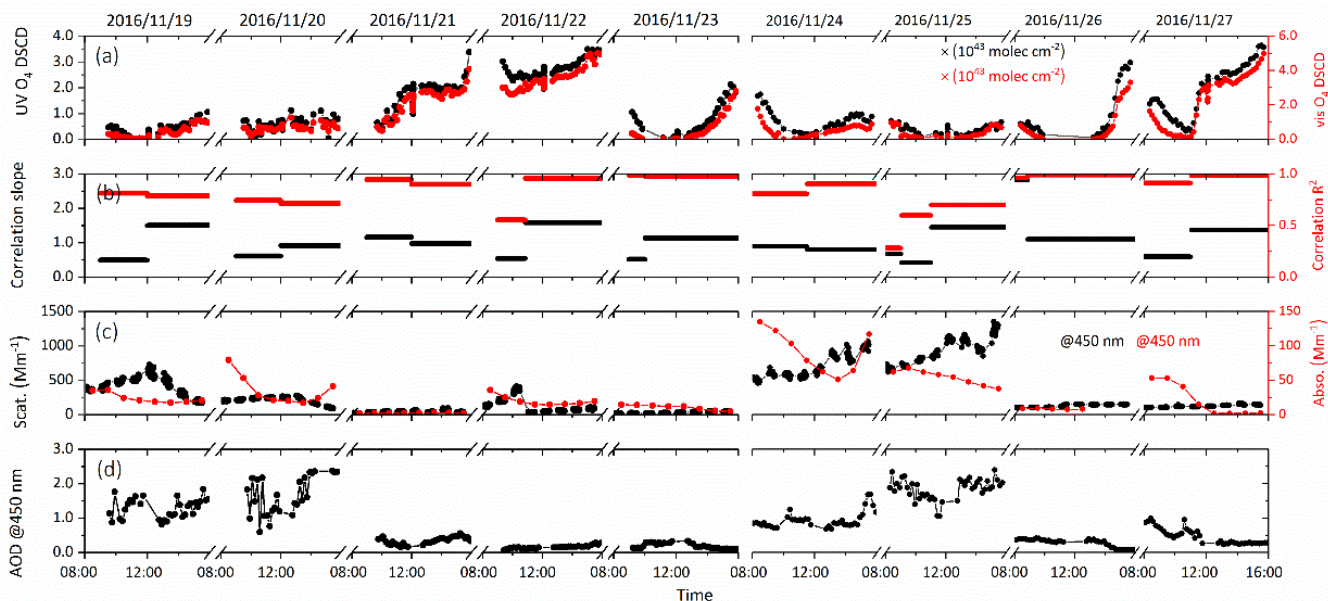
- (3) If the correlation slope floating around 1.0 and with a correlation R^2 of 0.75-0.85, we could know the weather mainly should be fog days. σ_{sca} and σ_{abs} are located at 450-1200 Mm^{-1} and 60-90 Mm^{-1} , while AODs are greater than 0.7.

Therefore, it represents the potential ability to determine the basic aerosol loading conditions from the MAX-DOAS observed O_4 absorptions.

4 Discussion

To investigate the feasibility and reliability, another short period MAX-DOAS measurement campaign operated in Gucheng, Hebei province (39.1382° N , 115.7163° E) from 19 to 27 November 2016 was used for the application of the new method to determine AOPs from O_4 absorptions. The MAX-DOAS instrument is the same as that one installed in CAMS. Due to absence of sunphotometer instrument, AODs at 450 nm were obtained by profiling the aerosol extinction coefficient based on MAX-DOAS measurements by utilizing the optimal estimation method (Frieß et al., 2006; Frieß et al., 2016; Xing et al., 2017). Besides, σ_{sca} and σ_{abs} were acquired using the co-located same integrating nephelometer (Aurora 1000, Ecotech) and 7-wavelength Aethalometer (AE-31, Magee Scientific), respectively. Moreover, the temporal resolution of σ_{sca} and σ_{abs} measurements are 1 minute and 1 hour, respectively.

Figure 7(a) and (b) shows the diurnal variations and segmental correlation of O_4 DSCDs in UV and visible bands during this campaign. According to the empirical relationships discussed in section 3.3, it can be inferred that the period segment during 09:00-11:00 in 25 November should be haze or heavy-haze ~~condition~~ weather type, because the UV and VIS O_4 DSCDs are all less than $0.5 \times 10^{43} \text{ molec cm}^{-2}$, and simultaneously the correlation slope and R^2 between them are 0.42 and 0.59, which are in line with the determination conditions that UV and visible O_4 DSCDs are mainly less than 1.1×10^{43} and $1.3 \times 10^{43} \text{ molec cm}^{-2}$, simultaneously combined the correlation slope and R^2 between them are mainly less than 0.6 and 0.8. Similarly, other periods that 09:00-12:00 of 21 Nov., 10:50-16:00 of 22 Nov., 10:00-15:00 of 23 Nov., 08:00-15:00 of 26 Nov. and 11:00-15:00 of 27 Nov. are mainly clear or ~~non~~light-haze weather type. And 09:00-10:00 of 19 Nov., 09:00-12:00 of 20 Nov. and 09:00-10:50 of 22 Nov. can be mainly regarded as haze or heavy-haze weather types.



325 **Figure 7. Time series of O₄ absorptions and aerosol optical properties at Gucheng, Hebei from 19 to 27 November 2016:**
 (a) UV and visible O₄ DSCDs, (b) correlation slopes and R² between O₄ DSCDs at 360.8 and 477.1 nm, (c) σ_{sca} and σ_{abs}
 at 450 nm, (d) AOD at 450 nm retrieved by MAX-DOAS.

330 Furthermore, the time series of in-situ σ_{sca} , σ_{abs} and MAX-DOAS retrieved AOD are shown in Fig.7 (c) and (d). According to the empirical relationships summarized above, the σ_{sca} , σ_{abs} and AOD are mainly located at 200-900 Mm⁻¹, 20-60 Mm⁻¹ and 0.9-2.5 under the haze segment of 09:00-11:00 of 25 November. Simultaneously, the in-situ measured σ_{sca} , σ_{abs} and MAX-DOAS retrieved AOD during the above same periods are ranged in 588.30-730.77 Mm⁻¹, 58.19-67.63 Mm⁻¹ and 1.39-2.22. The inferred results are in good agreement with the measured results, which are helpful to validate the AOPs determined according to the empirical relationships summarized above. The σ_{sca} , σ_{abs} and AOD are mainly located at 200-900 Mm⁻¹, 20-60 Mm⁻¹ and 0.9-2.5 under haze or heavy haze conditions, respectively. The in-situ σ_{sca} , σ_{abs} and MAX-DOAS retrieved AOD of the identified haze segment of 09:00-11:00 of 25 November are ranged in 588.30-730.77 Mm⁻¹, 58.19-67.63 Mm⁻¹ and 1.39-2.22. It indicates that the concluded empirical relationships can be used as the criterion to accurately determine the ranges of aerosol optical parameters of σ_{sca} , σ_{abs} and AOD. Nevertheless, we found two segments with correlation slopes > 1.0 and R² < 0.9 during 12:00-15:00 of 19 Nov. and 11:00-15:00 of 25 Nov., which is not included in cases of the empirical relationships. It suggests that more refined and quantitative relationships between aerosol optical parameters and O₄ absorptions need to be further achieved with the increases of the measured data, which can be established as a look up table, to retrieve the aerosol optical properties in the future.

340

Moreover, in order to illustrate the variations on the O₄ absorptions due to the change of aerosol loadings, we used radiative transfer model of SCIATRAN to simulate O₄ DSCDs in UV and Visible bands under conditions with different aerosol optical

345 properties. In total, 11 different aerosol scenarios were simulated and further the linear-regression analysis for the simulated UV and Visible O₄ DSCDs under different aerosol conditions were performed. The forward RTM simulation results presented in the Supplement (Table S2 and Figure S1) demonstrate that the O₄ absorptions information, including the value of UV and Visible O₄ DSCDs, the corresponding linear-regression slope and R² between them, could greatly reflect the variation of aerosol optical properties. More details can be referred in the Supplement.

350 **5 Summary and conclusions**

Ground-based MAX-DOAS measurements for O₄ DSCDs ~~in the at~~-UV and visible wavelength bands were carried out in Beijing from November 2016 to February 2017. Combined with the measured σ_{sca} and σ_{abs} and AOD, we have summarized the characteristics of O₄ absorptions and parameters of AOPs under different weather conditions during autumn-winter seasons. It was found that the averaged AOD increased from 0.311 in clear days to 1.338 in heavy-haze days. The averaged σ_{sca} changed dramatically from 44.524 Mm⁻¹ in ~~nonlight~~-haze days to 449.741 Mm⁻¹ in heavy-haze days. Moreover, the averaged σ_{abs} also obviously increased from 8.257 Mm⁻¹ in ~~nonlight~~-haze days to 53.257 Mm⁻¹ of heavy-haze ~~condition~~days to. Both the measured UV and visible O₄ DSCDs varied in the order of clear days > ~~nonlight~~-haze days > haze days > heavy-haze days > fog days. The corresponding correlation information (slope and R²) between O₄ DSCDs at UV and visible wavelength bands also changed synchronously when σ_{sca} and σ_{abs} have varied.

360 Considering the simultaneous variation of O₄ absorptions and AOPs, the segmental periods correlations analysis between UV and visible O₄ DSCDs were performed. Afterwards, the empirical relationships between O₄ absorptions and AOPs can be concluded for different aerosol loadings. It could be clear and ~~nonlight~~-haze days under the condition of linear-regression slopes correlation slopes are greater than 1.0 and R² mainly greater than 0.9, simultaneously, UV and Visible O₄ DSCDs are mainly greater than 2.5×10^{43} molec cm⁻². σ_{sca} , σ_{abs} and AOD are mainly less than 45 Mm⁻¹, 12 Mm⁻¹ and 0.4 under this condition, respectively. When the correlation slopes, R² and O₄ DSCDs are less than 0.6, 0.8 and 1.3×10^{43} molec cm⁻², respectively, it mainly should be haze or heavy-haze days. Under this condition, the σ_{sca} , σ_{abs} and AOD can be inferred to be mainly located at 200-900 Mm⁻¹, 20-60 Mm⁻¹ and 0.9-2.5, respectively. In addition, it should be fog days if the correlation slopes float around 1.0 and R² of 0.75-0.85. Another MAX-DOAS measurement campaign carried out at Gucheng from 19 to 27 November 2016 were used to validate the proposed new method, which could well determine the AOPs from the observed O₄ absorptions.

375 In this paper, we present a new method to deduce directly the parameters of aerosol optical properties from the observed UV and visible O₄ absorptions, which expands the usages of MAX-DOAS technique to fast semi-quantify the aerosol scattering and absorption properties. With the improvement of the look-up table, more precise and accurate inversion of aerosol optical properties can be achieved. Since only the O₄ DSCDs at elevation angle of 1° were employed to obtain the aerosol scattering and absorption at surface, it can be expected that vertical spatial-resolved of aerosol scattering and absorption can be retrieved by using O₄ DSCDs at different elevation angles in the future study.

Acknowledgements

This research was supported by grants from National Key Research and Development Program of China (2018YFC0213104, 2018YFC0213100, 2016YFC0203302, 2017YFC0210002), National Natural Science Foundation of China (41722501, 91544212, 51778596, 41575021), and Shanghai Pujiang Talent Program (17PJC015). We would like to thank CAMS and Peking University for the data of σ_{sca} and σ_{abs} measured in Gucheng and PKUERS, respectively.

References

- Allen, R. J., Sherwood, S. C., Norris, J. R., and Zender, C. S.: Recent Northern Hemisphere tropical expansion primarily driven by black carbon and tropospheric ozone, *Nature*, 485, 350-354, doi:10.1038/nature11097, 2012.
- Bergstrom, R. W., Pilewskie, P., Russell, P. B., Redemann, J., Bond, T. C., Quinn, P. K., and Sierau, B.: Spectral absorption properties of atmospheric aerosols, *Atmospheric Chemistry and Physics*, 7, 5937-5943, 2007.
- Che, H., Xia, X., Zhu, J., Wang, H., Wang, Y., Sun, J., Zhang, X., and Shi, G.: Aerosol optical properties under the condition of heavy haze over an urban site of Beijing, China, *Environmental science and pollution research international*, 22, 1043-1053, doi:10.1007/s11356-014-3415-5, 2015.
- Clémer, K., Van Roozendaal, M., Fayt, C., Hendrick, F., Hermans, C., Pinardi, G., Spurr, R., Wang, P., and De Mazière, M.: Multiple wavelength retrieval of tropospheric aerosol optical properties from MAX-DOAS measurements in Beijing, *Atmospheric Measurement Techniques*, 3, 863-878, 10.5194/amt-3-863-2010, 2010.
- Ding, A. J., Huang, X., Nie, W., Sun, J. N., Kerminen, V. M., Petäjä, T., Su, H., Cheng, Y. F., Yang, X. Q., Wang, M. H., Chi, X. G., Wang, J. P., Virkkula, A., Guo, W. D., Yuan, J., Wang, S. Y., Zhang, R. J., Wu, Y. F., Song, Y., Zhu, T., Zilitinkevich, S., Kulmala, M., and Fu, C. B.: Enhanced haze pollution by black carbon in megacities in China, *Geophysical Research Letters*, 43, 2873-2879, doi:10.1002/2016gl067745, 2016.
- Duan, L., Xiu, G., Feng, L., Cheng, N., and Wang, C.: The mercury species and their association with carbonaceous compositions, bromine and iodine in PM_{2.5} in Shanghai, *Chemosphere*, 146, 263-271, 10.1016/j.chemosphere.2015.11.058, 2016.
- Dubovik, O., Holben, B. R., Eck, T. F., Smirnov, A., Kaufman, Y. J., King, M. D., Tanre, D., and Slutsker, I.: Variability of Absorption and Optical Properties of Key Aerosol Types Observed in Worldwide Locations, *Journal of the Atmospheric Sciences*, 59, 590-607, 2001.
- Eck, T. F., Holben, B. N., Reid, J. S., O'Neill, N. T., Schafer, J. S., Dubovik, O., Smirnov, A., Yamasoe, M. A., and Artaxo, P.: High aerosol optical depth biomass burning events: A comparison of optical properties for different source regions, *Geophysical Research Letters*, 30, NO. 20, 2035, doi:10.1029/2003gl017861, 2003.
- Eck, T. F., Holben, B. N., Dubovik, O., Smirnov, A., Goloub, P., Chen, H. B., Chatenet, B., Gomes, L., Zhang, X. Y., Tsay, S. C., Ji, Q., Giles, D., and Slutsker, I.: Columnar aerosol optical properties at AERONET sites in central eastern Asia and

- aerosol transport to the tropical mid-Pacific, *Journal of Geophysical Research: Atmospheres*, 110, D06202, doi:10.1029/2004jd005274, 2005.
- Frieß, U., Monks, P. S., Remedios, J. J., Rozanov, A., Sinreich, R., Wagner, T., and Platt, U.: MAX-DOAS O₄measurements: A new technique to derive information on atmospheric aerosols: 2. Modeling studies, *Journal of Geophysical Research*, 111, doi:10.1029/2005jd006618, 2006.
- Frieß, U., Klein Baltink, H., Beirle, S., Clémer, K., Hendrick, F., Henzing, B., Irie, H., de Leeuw, G., Li, A., Moerman, M. M., van Roozendaal, M., Shaiganfar, R., Wagner, T., Wang, Y., Xie, P., Yilmaz, S., and Zieger, P.: Intercomparison of aerosol extinction profiles retrieved from MAX-DOAS measurements, *Atmospheric Measurement Techniques*, 9, 3205-3222, doi:10.5194/amt-9-3205-2016, 2016.
- Fyfe, J. C., Gillett, N. P., and Zwiers, F. W.: Overestimated global warming over the past 20 years, *Nature Climate Change*, 3, 767-769, 10.1038/nclimate1972, 2013.
- Galdos, M., Cavalett, O., Seabra, J. E. A., Nogueira, L. A. H., and Bonomi, A.: Trends in global warming and human health impacts related to Brazilian sugarcane ethanol production considering black carbon emissions, *Applied Energy*, 104, 576-582, 10.1016/j.apenergy.2012.11.002, 2013.
- Garland, R. M., Schmid, O., Nowak, A., Achtert, P., Wiedensohler, A., Gunthe, S. S., Takegawa, N., Kita, K., Kondo, Y., Hu, M., Shao, M., Zeng, L. M., Zhu, T., Andreae, M. O., and Pöschl, U.: Aerosol optical properties observed during Campaign of Air Quality Research in Beijing 2006 (CAREBeijing-2006): Characteristic differences between the inflow and outflow of Beijing city air, *Journal of Geophysical Research*, 114, doi:10.1029/2008jd010780, 2009.
- Guo, L., Guo, X., Fang, C., and Zhu, S.: Observation analysis on characteristics of formation, evolution and transition of a long-lasting severe fog and haze episode in North China, *Science China Earth Sciences*, 58, 329-344, doi:10.1007/s11430-014-4924-2, 2014.
- Hönninger, G., Friedeburg, C. v., and Platt, U.: Multi axis differential optical absorption spectroscopy (MAX-DOAS), *Atmospheric Chemistry and Physics*, 4, 231-254, 2004.
- He, X., L. C. C., Lau, A. K. H., Deng, Z. Z., Mao, J. T., Wang, M. H., and Liu, X. Y.: An intensive study of aerosol optical properties in Beijing urban area, *Atmospheric Chemistry and Physics*, 9, 8903-8915, 2009.
- Hess, M., Koepke, P., and Schult, I.: Optical Properties of Aerosols and Clouds: The Software Package OPAC *Bull. Amer. Meteor. Soc.*, 79, 831-844, 1998.
- Hönninger, G., and Platt, U.: Observations of BrO and its vertical distribution during surface ozone depletion at Alert, *Atmospheric Environment*, 36, 2481-2489, 2002.
- Huang, R. J., Zhang, Y., Bozzetti, C., Ho, K. F., Cao, J. J., Han, Y., Daellenbach, K. R., Slowik, J. G., Platt, S. M., Canonaco, F., Zotter, P., Wolf, R., Pieber, S. M., Bruns, E. A., Crippa, M., Ciarelli, G., Piazzalunga, A., Schwikowski, M., Abbaszade, G., Schnelle-Kreis, J., Zimmermann, R., An, Z., Szidat, S., Baltensperger, U., El Haddad, I., and Prevot, A. S.: High secondary aerosol contribution to particulate pollution during haze events in China, *Nature*, 514, 218-222, 10.1038/nature13774, 2014.

- Hytch, M. J., Putaux, J. L., and Penisson, J. M.: Measurement of the displacement field of dislocations to 0.03 Å by electron microscopy, *Nature*, 423, 270-273, doi:10.1038/nature01638, 2003.
- Karanasiou, A., Moreno, N., Moreno, T., Viana, M., de Leeuw, F., and Querol, X.: Health effects from Sahara dust episodes
 445 in Europe: literature review and research gaps, *Environment international*, 47, 107-114, 10.1016/j.envint.2012.06.012, 2012.
- Kaufman, Y. J., Tanré, D., Dubovik, O., Karnieli, A., and Remer, L. A.: Absorption of sunlight by dust as inferred from satellite and ground-based remote sensing, *Geophysical Research Letters*, 28, 1479-1482, doi:10.1029/2000gl012647, 2001.
- Kim, D., and Ramanathan, V.: Solar radiation budget and radiative forcing due to aerosols and clouds, *Journal of Geophysical Research*, 113, doi:10.1029/2007jd008434, 2008.
- 450 Lee, H., Irie, H., Gu, M., Kim, J., and Hwang, J.: Remote sensing of tropospheric aerosol using UV MAX-DOAS during hazy conditions in winter: Utilization of O₄ Absorption bands at wavelength intervals of 338–368 and 367–393 nm, *Atmospheric Environment*, 45, 5760-5769, 10.1016/j.atmosenv.2011.07.019, 2011.
- Levy, H., Horowitz, L. W., Schwarzkopf, M. D., Ming, Y., Golaz, J.-C., Naik, V., and Ramaswamy, V.: The roles of aerosol direct and indirect effects in past and future climate change, *Journal of Geophysical Research: Atmospheres*, 118, 4521-4532,
 455 doi:10.1002/jgrd.50192, 2013.
- Liou, S. C., Penner, J. E., Chuang, C., Walton, J. J., Eddleman, H., and Cachier, H.: A global three-dimensional model study of carbonaceous aerosols, in: *Journal of Geophysical Research: Atmospheres*, D14, 19411-19432, 1996.
- Platt, U., and Stutz, J.: Differential Optical Absorption Spectroscopy, 3, 540-75776, 2008.
- Ramana, M. V., Ramanathan, V., Feng, Y., Yoon, S. C., Kim, S. W., Carmichael, G. R., and Schauer, J. J.: Warming influenced
 460 by the ratio of black carbon to sulphate and the black-carbon source, *Nature Geoscience*, 3, 542-545, 10.1038/ngeo918, 2010.
- Ramanathan, V., Ramana, M. V., Roberts, G., Kim, D., Corrigan, C., Chung, C., and Winker, D.: Warming trends in Asia amplified by brown cloud solar absorption, *Nature*, 448, 575-578, doi:10.1038/nature06019, 2007.
- Remer, L. A., and Kaufman, Y. J.: Dynamic aerosol model: Urban/industrial aerosol, *Journal of Geophysical Research: Atmospheres*, 103, 13859-13871, doi:10.1029/98jd00994, 1998.
- 465 Seinfeld, J. H., and Pandis, S. N.: *Atmospheric chemistry and physics : from air pollution to climate change*, 2006.
- Shen, Y., Virkkula, A., Ding, A., Wang, J., Chi, X., Nie, W., Qi, X., Huang, X., Liu, Q., Zheng, L., Xu, Z., Petäjä, T., Aalto, P. P., Fu, C., and Kulmala, M.: Aerosol optical properties at SORPES in Nanjing, east China, *Atmospheric Chemistry and Physics*, 18, 5265-5292, doi:10.5194/acp-18-5265-2018, 2018.
- Tanré, D., Remer, L. A., Kaufman, Y. J., Mattoo, S., Hobbs, P. V., Livingston, J. M., Russell, P. B., and Smirnov, A.: Retrieval
 470 of aerosol optical thickness and size distribution over ocean from the MODIS airborne simulator during TARFOX, *Journal of Geophysical Research: Atmospheres*, 104, 2261-2278, doi:10.1029/1998jd200077, 1999.
- Thalman, R., and Volkamer, R.: Temperature dependent absorption cross-sections of O₂-O₂ collision pairs between 340 and 630 nm and at atmospherically relevant pressure, *Physical chemistry chemical physics : PCCP*, 15, 15371-15381, doi:10.1039/c3cp50968k, 2013.

- 475 Viana, M., Pey, J., Querol, X., Alastuey, A., de Leeuw, F., and Lukewille, A.: Natural sources of atmospheric aerosols influencing air quality across Europe, *The Science of the total environment*, 472, 825-833, doi:10.1016/j.scitotenv.2013.11.140, 2014.
- Wagner, T., Dix, B., Friedeburg, C. v., Frieß, U., Sanghavi, S., Sinreich, R., and Platt, U.: MAX-DOAS O₄measurements: A new technique to derive information on atmospheric aerosols-Principles and information content, *Journal of Geophysical Research: Atmospheres*, 109, D22205, doi:10.1029/2004jd004904, 2004.
- 480 Wang, S., Cuevas, C. A., Frieß, U., and Saiz-Lopez, A.: MAX-DOAS retrieval of aerosol extinction properties in Madrid, Spain, *Atmos. Meas. Tech.*, 9, 5089-5101, doi: 10.5194/amt-9-5089-2016, 2016.
- Wang, Z., Huang, X., and Ding, A.: Dome effect of black carbon and its key influencing factors: a one-dimensional modelling study, *Atmospheric Chemistry and Physics*, 18, 2821-2834, doi:10.5194/acp-18-2821-2018, 2018.
- 485 Weinzierl, B., Sauer, D., Esselborn, M., Petzold, A., Veira, A., Rose, M., Mund, S., Wirth, M., Ansmann, A., Tesche, M., Gross, S., and Freudenthaler, V.: Microphysical and optical properties of dust and tropical biomass burning aerosol layers in the Cape Verde region an overview of the airborne in situ and lidar measurements during SAMUM-2, *Tellus B: Chemical and Physical Meteorology*, 63, 589-618, doi:10.1111/j.1600-0889.2011.00566.x, 2017.
- Wilcox, E. M., Thomas, R. M., Praveen, P. S., Pistone, K., Bender, F. A., and Ramanathan, V.: Black carbon solar absorption suppresses turbulence in the atmospheric boundary layer, *Proceedings of the National Academy of Sciences of the United States of America*, 113, 11794-11799, doi:10.1073/pnas.1525746113, 2016.
- 490 Wittrock, F., Oetjen, H., Richter, A., Fietkau, S., Medeke, T., Rozanov, A., and Burrows, J. P.: MAX-DOAS measurements of atmospheric trace gases in Ny-Alesund - Radiative transfer studies and their application, *Atmospheric Chemistry and Physics*, 4, 955-966, 2004.
- 495 Xing, C., Liu, C., Wang, S., Chan, K. L., Gao, Y., Huang, X., Su, W., Zhang, C., Dong, Y., and Fan, G.: Observations of the vertical distributions of summertime atmospheric pollutants and the corresponding ozone production in Shanghai, China, *Atmos. Chem. Phys.*, 17, 14275-14289, doi.org/10.5194/acp-17-14275-2017, 2017.
- Yoon, S.-C., and Kim, J.: Influences of relative humidity on aerosol optical properties and aerosol radiative forcing during ACE-Asia, *Atmospheric Environment*, 40, 4328-4338, doi:10.1016/j.atmosenv.2006.03.036, 2006.
- 500 Yu, X., Zhu, B., Yin, Y., Yang, J., Li, Y., and Bu, X.: A comparative analysis of aerosol properties in dust and haze-fog days in a Chinese urban region, *Atmospheric Research*, 99, 241-247, doi:10.1016/j.atmosres.2010.10.015, 2011.
- Yu, X., Kumar, K. R., Lu, R., and Ma, J.: Changes in column aerosol optical properties during extreme haze-fog episodes in January 2013 over urban Beijing, *Environmental pollution*, 210, 217-226, doi:10.1016/j.envpol.2015.12.021, 2016.
- Zheng, G. J., Duan, F. K., Su, H., Ma, Y. L., Cheng, Y., Zheng, B., Zhang, Q., Huang, T., Kimoto, T., Chang, D., Pöschl, U., 505 Cheng, Y. F., and He, K. B.: Exploring the severe winter haze in Beijing: the impact of synoptic weather, regional transport and heterogeneous reactions, *Atmospheric Chemistry and Physics*, 15, 2969-2983, doi:10.5194/acp-15-2969-2015, 2015.